Energy Conversion and Management 322 (2024) 119182

Contents lists available at ScienceDirect

Energy Conversion and Management

journal homepage: www.elsevier.com/locate/enconman

Research Paper

Wind-coupled hydrogen integration for commercial greenhouse food and power production: A case study

Kayes Md Abu Reza, David S-K Ting, Rupp Carriveau *

Turbulence & Energy Laboratory, University of Windsor, Ontario, Canada

A R T I C L E I N F O

Keywords:
Green hydrogen
Electrolysis
Combined heat and power engines
Levelized cost of hydrogen
Payback period
Internal rate of return
Discounted payback period

A B S T R A C T

This study investigates the feasibility of using green hydrogen technology produced via Proton Exchange Membrane (PEM) electrolysis powered by a 200 MW wind farm for a commercial Greenhouse in Ontario, Canada. Nine different scenarios are analyzed, exploring various approaches to hydrogen (H_2) production, transportation, and utilization for electricity generation. The aim is to transition from using natural gas to using varying combinations of H_2 and natural gas that include 10 %, 20 %, and 100 % of H_2 with 90 %, 80 %, and 0 % of natural gas, to generate 13.3 MW from Combined Heat and Power (CHP) engines. The techno-economic parameters considered for the study are the levelized cost of hydrogen (LCOH), payback period (PBT), internal rate of return (IRR), and discounted payback period (DPB). The study found that a 10 % H_2-Natural Gas blend using existing wired or transmission line (W-10H_2) with 5 days of storage capacity and 2,190 h of CHP operation per year had the lowest cost with a LCOH of USD 3.69/kg. However, 100 % of H_2 using existing wired or transmission line (W-100H_2) with the same storage and operation hours revealed better PBT, IRR, and DPB with values of 6.205 years, 15.16 % and 7.993 years respectively. It was found impractical to build a new pipeline or transport H_2 via tube trailer from wind farm site to greenhouse. A sensitivity analysis was also conducted to understand what factors affect the LCOH value the most.

1. Introduction

In its 2018 report "Global Warming of 1.5 °C," the Intergovernmental Panel on Climate Change (IPCC) emphasized the necessity of reducing CO_2 emissions to zero by 2050 to restrict the global temperature increase to 1.5 °C above pre-industrial levels [1]. The advancement of technology and economic growth, contributing to elevated living standards in places around the world, has coincided with a significant rise in the production and emission of greenhouse gases detrimental to the environment [2]. As per the International Energy Agency (IEA), in 2023, global energy-related CO_2 emissions grew by 1.1 %, increasing 410 million tonnes (Mt) to reach a new record high of 37.4 billion tonnes (Gt) [3].

Hydrogen is increasingly recognized as a potent tool to help achieve the objective of reducing and ultimately phasing out a reliance on fossil fuels, aligning with the objectives of the REPowerEU initiatives (European Commission, 2022). The International Energy Agency (IEA) anticipates the completion of 68 "demonstration projects" within the hydrogen sector by 2030, with several projects already operational (IEA, 2022b) [2]. Serving as a versatile energy carrier, hydrogen plays a crucial role in ensuring the sustainability of future decarbonized energy systems on a global level.

Depending on the production process and primary power source, hydrogen is often classified by colors [4]. Table 1 shows the comparison among the common colors of hydrogen including the costing and CO_2 emission [5]. "Blue" hydrogen is produced through the steam methane reforming of natural gas, a process that yields hydrogen and carbon dioxide. While the CO_2 is intended to be sequestered underground in this method through carbon capture system (CCS) to reduce Greenhouse gases (GHG) emission [4,5]. In contrast, "grey" hydrogen is also derived from a method similar to blue hydrogen; however, the resulting carbon dioxide is not sequestered but released directly into the atmosphere [4,5]. "Brown" hydrogen, the most prevalent form, is created from a feedstock rich in hydrocarbons through gasification, yet it emits substantial levels of CO_2 into the atmosphere [5]. Meanwhile, "black" hydrogen is obtained via coal gasification, with hydrogen being isolated from other gases through specific membranes or absorption processes, but the excess gases are emitted into the atmosphere [5]. Other less common hydrogen colors include purple which is generally identified as electrolytic hydrogen generated by nuclear power [6]. Turquoise hydrogen involves less common techniques like microwave plasmalysis

* Corresponding author.
E-mail address: rupp@uwindsor.ca (R. Carriveau).

https://doi.org/10.1016/j.enconman.2024.119182
Received 16 July 2024; Received in revised form 17 October 2024; Accepted 18 October 2024
Available online 28 October 2024

Nomenclature

AE	Alkaline Electrolyzer
C	Cost (USD)
C_0	Initial Investment or CAPEX Cost (USD)
CAPEX	Capital Expenditure (USD)
CF_a	Annual Cash Flow (USD/yr)
CF_t	Cash Flow in time "t" (USD/yr)
CHP	Combined Heat and Power Engine
D	Diameter of Pipeline (m)
DPB	Discounted Payback Period (yrs)
g	Gravity (m/s^2)
hr	Hour
HWB	Hot Water Boiler
IRR	Internal Rate of Return (%)
kWh	Kilo Watt Hour
L	Length of Pipeline (m)
LCOH	Levelized Cost of Hydrogen (USD/kg)
LHV	Lower Heating Value (MJ/m^3) or (MJ/kg) in terms of volumetric and gravimetric respectively
M	Million
$\dot{m}$	Mass Flow Rate of H_2 (kg/s)
M_{H_2}	Hydrogen production in (kg/yr)
MJ	Mega Joule
MW	Mega Watt
NG	Natural Gas
NPV	Net Present Value (USD)
OH	Annual operating hour (hrs/yr)
OH-2190	2,190 h of operation for CHP engines per year
OH-1,010	1,010 h of operation for CHP engines per year
O&M	Operation & Maintenance
P_1	Inlet Pressure (bar)
P_2	Outlet Pressure (bar)
P	Pipeline
PBT	Payback Period (yrs)
PEM	Proton Exchange Membrane
r	Discount Rate (%)
R	Gas Constant ($Jmol^{-1}K^{-1}$)
SOE	Solid Oxide Electrolyzer
t	Specified Time (yr)
T	Temperature (K) or Maximum Time (yr)
T	Trucking/Tube Trailer
W	Wired/Existing Grid/Existing Transmission Line
yr	Year
Z	Compressibility Factor

Subscripts and Superscripts

blend	Blending
comp	Compressor
el	Electrolyzer
elec pur	Electricity Purchase
pipe	Pipeline Installation
stack repl	Stack Replacement
tank	H_2 Storage Tank
trail	Tube Trailer

Greek Letters

λ	Friction Coefficient
Δh	Elevation Level Difference (m)

that use methane as a feedstock and separate the carbon out as a solid powder [6]. White hydrogen is considered by many as "natural" hydrogen that is found at great depths > 3000 m in the earth [7].

Conversely, "green" hydrogen is considered by many a more sustainable alternative, as it can be generated from renewable sources of water and electricity via electrolysis, where electricity is generated from renewable sources such as wind, hydro or solar power [5,8]. Electrolysis involves the splitting of water into hydrogen and oxygen using electricity and results in no carbon emissions.

Green hydrogen is gaining importance in the global energy mix due to its ability to help solve critical issues like energy security, sustainable development, and the climate at large. Green hydrogen is produced by electrolyzing water with renewable energy sources, resulting in no greenhouse gas emissions. Its integration into the energy mix can help reduce reliance on fossil fuels and cut the emissions driving climate change [8]. It can be stored and transported, offering a solution for energy storage and grid stability, particularly as the use of intermittent renewable energy sources grows.

Fig. 1 compares specific energy (energy per mass or gravimetric density) and energy density (energy per volume or volumetric density) for several fuels based on lower heating values from the literature [9]. When comparing energy content by mass, hydrogen has almost triple the amount of energy compared to gasoline, delivering 120 MJ/kg for hydrogen, against 44 MJ/kg for gasoline. However, when measured by

Table 1
Common hydrogen color shades, technology, cost, and carbon dioxide emissions.

Hydrogen Colour	Production Technology	Cost	CO_2 Emission (kg/kg of H_2)
Green	Electrolysis of water using renewable energy sources	High	Zero
Blue	Steam reforming of natural gas, with carbon capture and storage	Moderate	9–12
Grey	Steam reforming of natural gas, without carbon capture and storage	Low	16–18
Brown	Gasification of coal or another hydrocarbon-rich feedstock	Moderate	19–25
Black	Coal gasification, with hydrogen separation and other gases released into the atmosphere	High	24–28

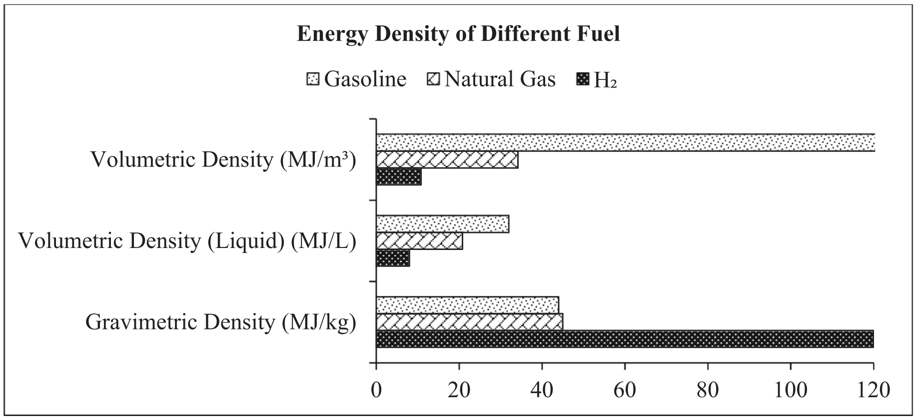

Fig. 1. Energy densities of different fuel based on Lower Heating Value (LHV).

volume, the scenario is flipped; liquid hydrogen has an energy density of 8 MJ/L, while gasoline boasts a higher energy density of 32 MJ/L [9].

Hydrogen is characterized by a density of 0.0899 kg/m^3 at standard temperature and pressure (STP) i.e. 0 °C and 1 atm pressure. Additionally, it retains its liquid state at a very low boiling point of −252.87 °C when under 1 atmosphere of pressure [10,11]. By compressing the gaseous hydrogen up to 700 bar, the volumetric density will be significantly changed and so is the volumetric energy content in terms of lower heating value (LHV). Table 2 shows the comparison of hydrogen mass density and energy density (LHV) at different pressure and state [12]. The LHV of Hydrogen exhibited a remarkable increase, rising from 10.8 MJ/m^3 at 1 atm to an impressive 7,452 MJ/m^3 at 700 bar, demonstrating a substantial leap. This property underscores the considerable advantages of hydrogen in both volumetric and gravimetric heat content, suggesting a promising future for hydrogen as a superior energy carrier.

Green hydrogen can be used to generate electricity or heat, making it a versatile energy source [5]. Certain sectors like heavy transport, aviation, and steel manufacturing are challenging to decarbonize with current renewable energy technologies. Green hydrogen provides a low-carbon alternative for these hard-to-abate industries [8]. Producing green hydrogen from local renewable sources reduces dependence on imported fossil fuels, increasing energy security and reducing geopolitical risks. It also leads to a more diverse and resilient energy infrastructure [5]. The development of green hydrogen technologies can drive innovation, economic growth, and create new job opportunities as countries build the necessary infrastructure for its production, storage, and transportation [8].

2. Study objectives and novelty

This study provides a detailed techno-economic assessment of nine distinct scenarios, where a wind farm powers a commercial greenhouse operation located 26 km apart. The wind farm has capacity to generate 200 MW of electrical power, which is integrated into the existing transmission grid. In contrast, the commercial greenhouse is equipped with four natural gas-fired Combined Heat and Power (CHP) engines, each with a generation potential of 3.3 MW, and five natural gas fired hot water boilers, each offering a substantial thermal output of 8,830 kW. These installations not only fulfill the greenhouse's energy demands, ensuring an optimal growth environment for the plants, but also facilitate delivery of surplus electricity per a Provincial power sales contract.

Southwestern Ontario has the greatest concentration of commercial greenhouses in North America. Nearly 4000 acres of Ontario greenhouses produce over 521million kg of fresh produce generating farmgate values over $1 billion USD through Canadian consumption and American export [13]. This economically critical sector in Ontario is a massive consumer of electricity and natural gas. Single operations using grow lights can pull loads of 50 MW. In this particular study the Leamington area Greenhouse has 25 acres of size with a significant of energy demand. There is significant interest in finding more available and sustainable energy pathways for growers as this sector looks to expand. This strong interest was the origin of this study. As several factors such as geographic and climatic conditions, access to renewable energy sources and hydrogen production facilities, regulatory frameworks, the scale and type of greenhouse operations may influence, this area is of great importance to integrate green hydrogen. However, several factors may influence the transferability of our results to different contexts such as geographic and climatic conditions, existing energy infrastructure in other regions, including access to renewable energy sources and hydrogen production facilities, regulatory frameworks, the scale and type of greenhouse operations.

The core objective of this study is to transition the greenhouse's energy generation from natural gas-fired CHP engines to a more sustainable solution employing hydrogen, either in its pure form or as part of a hydrogen-natural gas blend. This study explores three different levels of demand which are classified as low (10 % hydrogen, 90 % natural gas = 10H_2), medium (20 % hydrogen, 80 % natural gas = 20H_2), and high (100 % hydrogen = 100H_2) and then integrates them into three overarching delivery scenarios. Table 3 delineates these nine case scenarios. The delivery scenarios are as follows: the 'Wired/Existing Grid' scenario, where hydrogen production, storage, and blending facilities are installed directly at the greenhouse premises (identified as W-10H_2, W-20H_2, and W-100H_2); the 'Trucking' scenario, where hydrogen is produced and compressed at the wind farm, then transported to the greenhouse via truck or tube trailer for storage and blending (referred to as T-10H_2, T-20H_2, and T-100H_2); and the 'Pipeline' scenario, where hydrogen is also produced at the wind farm but conveyed through a pipeline to the greenhouse for subsequent storage and blending (denoted as P-10H_2, P-20H_2, and P-100H_2). The decision

Table 2
Comparison of state of hydrogen.

State of H_2	Mass Density (kg/m^3)	Gravimetric Energy Density (MJ/kg)	Volumetric Energy Density (MJ/m^3)
At STP	0.0899	120	10.8
At 0°C and 30 bar	2.593	120	311
At 0°C and 300 bar	26.6	120	3,192
At 0°C and 500 bar	44.4	120	5,328
At 0°C and 700 bar	62.1	120	7,452
Liquid H_2	70.8	120	8,496

Table 3
Case scenarios.

Case Scenarios Wired/Existing Grid 1	2	3	Trucking 4	5	6	Pipeline 7	8	9
W-10H_2	W-20H_2	W-100H_2	T-10H_2	T-20H_2	T-100H_2	P-10H_2	P-20H_2	P-100H_2

to analyze nine scenarios was driven by the need to assess feasible options for hydrogen production and transportation, given the 26 km distance between the wind farm and the greenhouse.

The research is built on extensive data collection from both the wind farm and greenhouse, covering aspects such as electricity generation, thermal and electrical needs of the greenhouse, auxiliary power consumption of the CHP engines, and fuel usage for boilers and engines. Utilizing this data, a comprehensive model has been developed to ascertain the requirements for hydrogen, power, and demineralized water for each scenario, aiming to achieve a 13.3 MW electricity output from the CHP engines. These engines provide heat to the greenhouse when operating and fulfill the greenhouse owner's electricity delivery contract obligations with Ontario's Independent Electricity System Operator (IESO).

The study considers engine model and capacity, production systems i.e. electrolyzer, compressor, storage media and storage capacities, tube trailer capabilities, and pipeline sizing for each individual case. The analysis also requires market prices for equipment and systems, power purchase and selling rates, and other economic factors such as the duration of analysis and discount rate. To check the feasibility of the nine cases mentioned above, a techno-economic evaluation is conducted. Numerous studies, including those referenced in [1,14–17], have employed metrics such as levelized cost of hydrogen (LCOH), internal rate of return (IRR), payback period (PBT), and discounted payback period (DPB) to perform techno-economic analyses of various green hydrogen production and utilization technologies. Accordingly, the primary objective of our study is to evaluate the techno-economic viability of nine cases using financial metrics, including LCOH, PBT, DPB, and IRR. Fig. 2 shows the methodology used in this study.

Prior research has been conducted on hydrogen production from offshore, onshore, or dedicated wind power using a variety of electrolyzers and its applications in fields such as hydrogen fuel cells, compression, storage, transportation, liquid organic hydrogen carriers (LOHC), methanation, blending with natural gas for industrial use, residential heating, combi boilers, and steel manufacturing industries.

This study stands out as a comprehensive analysis of hydrogen-integrated greenhouse horticulture along with the power generation via hydrogen or H_2-NG blend fired CHP engines, assessing its energy practical sustainability with techno-economic viability, something not yet obviously discovered in the literature.

3. Literature review

This study includes green H2 production, storage, compression, transportation through pipeline and tube trailer (trucking), blending with NG, producing electricity and heat from CHP engine to provide necessary heat and power in greenhouse with exporting the surplus energy to grid. Considering all these items, Table 4 shows an overview of studied literatures.

In 2020, Ozturk et al. [18] introduced a new integrated system that blends hydrogen and natural gas for residential heating and cooking with combi boiler and gas stove.

Several studies were conducted in 2021. Franco et al. [1] conducted a techno-economic assessment on the different pathways that includes onshore and/or offshore H_2 production, conversion to different H_2 carriers and transportation by pipeline or ship to the import terminal. Among the pathways studied, the use of pipelines to transport hydrogen shows as the best solution having LCOH of €5.35/kgH_2. Tebibel et al. [19] presents a multi-objective optimization approach for a wind-hydrogen production system (WHPS) by integrating wind turbines, a water electrolyzer, battery bank, power converters, and a hydrogen tank to minimize total hydrogen deficit, energy dump possibility, levelized cost of hydrogen, CO_2 emission avoided, and natural gas preserved having LCOH of $33.70/kg. Dinh et al. [14] introduced a new model that includes calculations for wind power output, electrolyzer plant size, and hydrogen production based on varying wind speeds. By applying Discounted Payback and Net Present Value analyses, the study evaluated the economic feasibility of a hypothetical offshore wind farm, demonstrating profitability at a hydrogen price of €5/kg with different storage capacities.

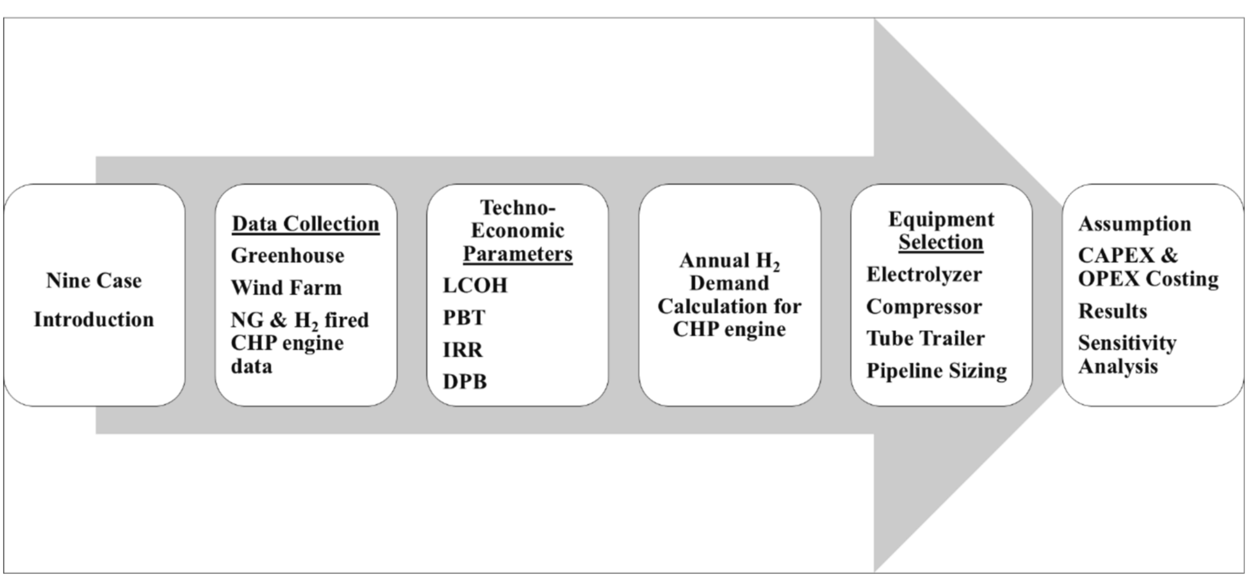

Fig. 2. Methodology of the study.

Table 4
Overview of literature.

Reference Paper	Year	Renewable Sources	Electrolysis	H_2 Storage	H_2 Compression	H_2 Transportation through Trucking	H_2 Transportation through Pipeline	H2 Blending with NG	Heat/Power Producing Components	Application/CHP for Greenhouse	Research Objective	Techno-economic Parameters Considered
Ozturk et al. [18]	2020	−PV panels −Wind turbines	Alkaline	✓			✓	✓	Combi boiler, gas stove	Residential heating and cooking	–H_2 production and CO_2 reduction −Energy and exergy efficiency	Energy and exergy efficiency.
Franco et al. [1]	2021	Wind farm	−PEM −Alkaline	✓	✓		✓			–NH_3 conversion −LOHC conversion −Ship/vessel	Techno-economic Assessment	LCOH, NPV, and energy expenditure.
Tebibel et al. [19]	2021	−Wind Turbine −Battery Bank	Alkaline	✓						Fertilizer and Glass Industry	Multi-objective optimization of wind-hydrogen production system (WHPS)	THD, LCOH, EDP, CO_2 emission.
Dinh et al. [14]	2021	Offshore Wind Farm	PEM	✓		✓					Viability assessment of hydrogen production	H_2 production cost, DPB, NPV.
Sorgulu et al. [20]	2022	−PV panels −Off-grid &On-grid wind turbines	Generalized	✓			✓	✓	Combi boiler, gas stove, fuel cell	Residential heating and cooking, electricity	Thermodynamic analysis and techno-economic assessment	Net present cost, energy and exergy efficiencies.
Lucas et al. [16]	2022	WindFloat Atlantic Wind Farm	PEM	✓	✓		✓				Feasibility of hydrogen production	H_2 production cost & selling rate.
Jang et al. [21]	2022	Offshore wind power	PEM				✓				Techno-economic analysis and Monte Carlo simulation	H_2 production cost and NPV
Lamagna et al. [22]	2022	Offshore Wind Power	SOEC						Solid Oxide Fuel Cell −(SOFC) & (rSOC)		H_2 production for Fuel cell or export.	Produced H_2 and power
Benalcazar and Komorowska [23]	2022	−PV −Onshore wind Power	PEM								Techno-economic analysis and Monte Carlo simulation	LCOH
Groenemans et al. [24]	2022	Offshore wind power	PEM	✓	✓	✓					Techno-economic analysis	LCOH
Luo et al. [25]	2022	Offshore wind power	PEM SOEAE	✓			✓			Refueling, industrial O_2	Analyze the methods of hydrogen production	H_2 production cost
Nasser et al. [26]	2022	−Wind Turbine −PV Panel	Alkaline	✓	✓						Techno-economic assessment	H_2 production cost, overall system efficiency
Costa et al. [2]	2023	−Wind power −PV cell	Alkaline					✓	−Boiler −CHP engine	Methanator, CO_2 capture, Industry, Building, Transport	Techno-economic assessment	Payback Period
Egeland-Eriksen et al. [27]	2023	−Offshore and onshore wind turbine −Lithium-ion battery	PEM	✓	✓						Simulating offshore hydrogen production	H_2 production cost, overall system efficiency

(continued on next page)

Table 4 (*continued*)

Reference Paper	Year	Renewable Sources	Electrolysis	H_2 Storage	H_2 Compression	H_2 Transportation through Trucking	H_2 Transportation through Pipeline	H2 Blending with NG	Heat/Power Producing Components	Application/CHP for Greenhouse	Research Objective	Techno-economic Parameters Considered
Superchi et al. [4]	2023	−Wind power −BESS	Alkaline								Feasibility of coupling the intermittent electric power generation	LCOH
Superchi et al. [28]	2023	−Wind farm −Grid −BESS	Alkaline	✓						Substitute the coke in EAF in steel manufacturing	Techno-economic analysis	LCOH, Green Index (GI), CO_2 reduction
Idriss et al. [29]	2023	Wind turbines	−Alkaline −PEM								Techno-Economic Potential	LCOH, CO_2 emission reduction, H_2 production amount
Akdag [30]	2023	Offshore Wind Technology (OWF)	PEM	✓			✓			H_2 fuel cell vehicle	Applicability to hydrogen fuel cell for vehicle	H_2 production cost
Cheng and Hughes [31]	2023	−Offshore wind power −Solar PV −Battery	PEM	✓						Transportation by ship	Least-cost optimization modelling	LCOH
Li et al. [17]	2023	−Wind Farm −PV −Battery	Generalized	✓	✓	✓				NH_3 production and storage	Techno-economic analysis	LCOH, NPV, Payback Period,
Kim et al. [32]	2023	Wind power	PEM	✓			✓				Feasibility and techno-economic study, optimization	H_2 production cost
Komorowska et al. [33]	2023	Wind Power	PEM								Evaluating the competitiveness and uncertainty of offshore wind-to-hydrogen production	LCOH
Nasser and Hassan [34]	2023	−PV panels −Wind turbines	−PEM −SOE	✓	✓						Techno-enviro-economic analysis	LCOH & system efficiency
Reyes-Bozo et al. [15]	2024	Grid assisted power from renewable energy through PPA	Alkaline	✓	✓			✓		−Refueling station − smelting and refining furnaces in Al recycling facilities	Techno-economic analysis	H_2 production, CO_2 reduction. NPV, IRR, and PBT
Makepeace et al. [35]	2024	−Wind farms −Solar PV	Generalized		✓	✓	✓			Ammonia, LOHC, H_2 Slush, liquefied hydrogen export	Techno-economic analysis	LCOH in different modes of production, transport & conversion
Giampieri et al. [36]	2024	Offshore Wind Power	PEM	✓	✓	✓	✓			Methylcyclohexane and ammonia	Techno-economic assessment	LCOH

(*continued on next page*)

Table 4 (*continued*)

Reference Paper	Year	Renewable Sources	Electrolysis	H_2 Storage	H_2 Compression	H_2 Transportation through Trucking	H_2 Transportation through Pipeline	H2 Blending with NG	Heat/Power Producing Components	Application/CHP for Greenhouse	Research Objective	Techno-economic Parameters Considered
										production, and storage		
Benalcazar and Komorowska [37]	2024	–Solar PV –Onshore Wind Farm	–PEM –Alkaline				✓				Techno-economic analysis and uncertainty assessment	LCOH
Gado [38]	2024	–Solar PV –Wind Power	PEM	✓	✓					Green Ammonia	Techno-economic-environmental assessment	LCOH
Hüner [39]	2024	Solar PV	PEM								Mathematical Modeling	H_2 Production Rate, Annual H_2 Production
Park et al. [40]	2024	Solar PVESS	Alkaline	✓							Techno-economic analysis, multi-objective optimization	LCOH, Annual H_2 Production (APOH)

Various investigations with techno-economic analysis of green hydrogen production technology associated with its transportation and usage were conducted in 2022. Sorgulu et al. [20] set up an experimental lab-scale system to supply a mixture of hydrogen and natural gas, as well as electricity, for a community of 100 houses for its heating, cooking and power consumption to find the net present costs, energy and exergy. Lucas et al. [16] explored the feasibility of using excess wind energy for green hydrogen production, focusing on the WindFloat Atlantic offshore wind farm. The study emphasizes the importance of optimizing the hydrogen plant power-to-wind farm capacity ratio for cost-effective hydrogen production. Jang et al. [21] examined the most cost-effective method for connecting offshore wind power plants to hydrogen production facilities, through a techno-economic analysis using net present value calculation, sensitivity analysis, and Monte Carlo simulation. The calculated H_2 production costs were \$13.81/kgH_2 for distributed production, \$13.85/kgH_2 for centralized production, and \$14.58/kgH_2 for onshore production.

Lamagna et al. [22] investigated the integration of a reversible Solid Oxide Cell (rSOC) with an offshore wind turbine for local energy management benefits. With the dynamic model simulation, controlled by an algorithm, the system can produce up to 15 tons of hydrogen with an export-based strategy. Benalcazar and Komorowska [23] focused on assessing the economic and technical factors affecting the success of Poland's green hydrogen strategy through the development of a Monte Carlo-based model. The study analyzed the economics of renewable hydrogen at different stages of technological development and market adoption by comparing the LCOH in some regions in 2020, 2030, and 2050. Groenemans et al. [24] compared two scenarios: producing hydrogen offshore and transporting it to shore via a gas pipeline and producing hydrogen onshore using electricity from an offshore wind farm. The analysis revealed that the offshore production method resulted in a lower LCOH of \$2.09/kg, and \$3.86/kg H_2 for offshore.

Luo et al. [25] discussed converting wind-generated electricity into hydrogen through water electrolysis for long-term storage to address increasing costs of offshore wind projects. They explored different methods of hydrogen production, highlighted economic analyses, and concluded that hydrogen production from offshore wind could become more cost-effective and feasible in the future. Nasser et al. [26] evaluated a hybrid renewable energy system using wind turbines and PV panels for hydrogen production and storage across different climates in five Egyptian cities in terms of energy storage, efficiency, and cost. Results show production costs varied from \$4.54/kg to \$7.48/kg.

Costa et al. [2] evaluated a setup for producing green hydrogen through electrolysis using renewable energy sources and capturing CO_2 from cogenerator exhaust gases They then used the captured CO_2 in a methanation reaction with hydrogen to produce synthetic methane. Economic analysis showed payback times below ten years, especially with hydromethane, indicating potential residential applications with small photovoltaic sizes. This study was among a group of even more recent works on green H_2 production and integration like Egeland-Eriksen et al. [27] that presented a model to simulate an energy system where electricity from an offshore wind turbine is considered over a 31-day period having a maximum of 17,242 kg of production, with the lowest production cost of \$4.53/kg.

Superchi et al. [4] explored the feasibility of integrating wind farm electricity with alkaline electrolyzers to produce green hydrogen. By coupling the model with historical wind farm data and using a sizing algorithm, they found the best combination between the actual wind farm power output and the electrolyzer capacity to reach the lowest LCOH possible. Superchi et al. [28] focused on using green hydrogen to decarbonize the steelmaking industry. By coupling an onshore wind farm with lithium-ion batteries and alkaline electrolyzers, the research conducts techno-economic analyses on various configurations to optimize the LCOH and Green Index (GI) with LCOH of around €6.5/kg. Idriss et al. [29] focused on producing hydrogen from wind energy in rural area using renewable energy and energy storage systems through an ecological analysis. They found the mass and the LCOH were 29.68 tons and \$11.48/kg for a region 18.68 tons and \$18.25/kg for another region respectively.

Akdag et al. [30] presented a comprehensive model examining hydrogen production, storage, and transportation, with a detailed techno-economic analysis projecting a decreasing cost of green hydrogen production over time. The estimated cost of producing green hydrogen is expected to decrease from €6.26/kg in 2023 to €1.13/kg by 2050, with overall hydrogen costs decreasing from €10.7/kg in 2023 to €2.42/kg in 2050. In their study, Cheng and Hughes [31] investigated the prospective contribution of offshore wind power to renewable hydrogen production in Australia by 2030. Utilizing wind and solar data along with wind turbine power curve inputs, they simulated hydrogen production through PEM electrolysis, yielding an estimated LCOH range of 4.4–5.5 AUD/kg H_2 for 2030. Li et al. [17] examined the techno-economic feasibility of a wind-photovoltaic-electrolysis-battery (WPEB) power system. The study indicates that the WPEB system outperforms the wind-photovoltaic-battery (WPB) system economically when hydrogen production exceeds 12,000 kg/day, where metrics such as NPV, IRR, LCOH, and PBT came in at 1781.22 million¥, 13.19 %, 13.1665¥/kg, 9 years respectively.

Kim et al. [32] highlights the potential of green H_2 production from a wind farm through optimization. The production costs ranged from \$1.64 to \$4.46 per kg of H_2. The analysis indicates that systems using alkaline electrolyzers can achieve feasible prices in certain regions compared to current green H_2 production costs. Komorowska et al. [33] developed a Monte Carlo-based framework to assess the competitiveness of offshore wind-to-hydrogen production, focusing on the variability of the LCOH and uncertainties in long-term planning in 2030 and 2050. Results indicate that offshore wind-based hydrogen could cost between €3.60 to €3.71/kg H_2 in 2030 and €2.05 to €2.15/kg H_2 in 2050. Nasser et al. [34] in 2023 evaluated hydrogen production systems using PEM and SOEC electrolyzers powered by various sources, including PV panels, wind turbines, waste heat recovery Rankine cycles, and grid electricity. The highest efficiency is achieved with waste heat systems (22.91 %), while LCOH ranges from \$1.19 to \$12.16/kg and LCOCH from \$5.03 to \$17.1/kg.

Most recently, Reyes-Bozo et al. [15] investigated the feasibility of using green hydrogen as a substitute for natural gas in aluminum recycling processes to reduce carbon emissions. The evaluation indicates that on-site green hydrogen generation offers a positive NPV of €57,370, an IRR of 9.83 %, and a payback period of 19.63 years with a significant reduction of CO_2 emission. Makepeace et al. [35] introduced a techno-economic model to demonstrate the feasibility of transporting green hydrogen globally along major regional routes using various mediums such as ammonia, LOHC, hydrogen slush, compressed or liquefied hydrogen, and different transportation modes like shipping, truck, train, and pipeline. A Monte Carlo-based technique is employed to evaluate the LCOH over the next 30 years, indicating that by 2050, around 85 % of the projected 300Mt of green H_2 demand will need to be transported between regions for the most economically optimal distribution.

Giampieri et al. [36] evaluated technical requirements and costs for green hydrogen production and transport via data analysis, technology selection, system design, and simulation models. The most cost-effective scenario for projects starting in 2025 involves compressed hydrogen production, but economic feasibility depends on storage period and distance to shore. Liquefied hydrogen and methylcyclohexane could become more cost-effective by 2050, potentially reducing the LCOH to around £2 per kilogram or lower.

Magne et al. [41] indicated that biomass, particularly from agriculture, could see its theoretical potential increase from 1,214 million tonnes in 2021 to 1,371 million tonnes by 2050. Transitioning to modern bioenergy could support decarbonization efforts, with bioelectricity contributing around 24 % to total electricity generation in 2021 and achieving global decarbonization by 2050. Najar et al. [42] discussed various waste sources and the challenges in valorizing them, emphasizing the role of thermophilic microbes in bioremediation. These microbes, known for their thermostability, can effectively convert waste into valuable products, supporting the development of a biocircular economy and advancing zero-carbon sustainable practices. Shen et al. [43] employed data mining to analyze the morphological and environmental characteristics of VCs and their cooling effects, using Nanjing as a case study. Findings indicate a significant correlation between VC characteristics and cooling, with temperature differences reaching up to 5.4 °C and cooling ranges between 13 and 600 m. Vahidhosseini et al. [44] highlighted the integration of solar energy technologies, heat pumps, and thermal energy storage systems to achieve net-zero and carbon–neutral buildings. It explores different thermal energy storage materials, including sensible, latent, and thermochemical storage, while evaluating their advantages and limitations.

Ma et al. [45] have shown that photovoltaic thermal (PVT) systems can effectively complement PEMEs by providing necessary thermal energy, thus improving overall system performance. Research indicates that various environmental factors, such as irradiation intensity, ambient temperature, and inlet flow rate, significantly influence the efficiency of solar PVT coupled PEM electrolyzer system. Asianban et al. [46] have focused on developing simplified models that accurately represent the dynamic responses of PEM electrolyzers, enabling flexibility studies within power systems given the intermittent nature of RESs, precise modeling of PEM electrolyzers. Validation against both static and dynamic experimental data demonstrates the model's effectiveness, achieving an average error of 0.66 % in static conditions and 3.93 % in dynamic scenarios. Benghanem et al. [47] have explored the performance of two prominent PEM and Alkaline Water Electrolyzers powered by photovoltaic (PV) systems. Findings indicate that PEM electrolyzers require lower voltage to produce equivalent hydrogen amounts compared to AWE.

4. Nine case introduction

The study delineates nine distinct scenarios, which are grouped into three principal modalities: integration with the existing electrical grid, hydrogen transportation via trucking, and pipeline delivery. Illustrated in Fig. 3 are scenarios W-10H_2, W-20H_2, and W-100H_2, which involve hydrogen production utilizing power from the central grid, with the hydrogen being generated at 30 bar. This hydrogen is then stored and blended within the vicinity of the greenhouse at varying ratios: 10 %, 20 %, and 100 % hydrogen to 90 %, 80 %, and 0 % natural gas, respectively.

Fig. 4 presents the T-10H_2, T-20H_2, and T-100H_2 scenarios, where hydrogen is produced at wind farm sites, compressed to 500 bar, and conveyed to the greenhouse area by tube trailers for storage and blending operations.

The P-10H_2, P-20H_2, and P-100H_2 scenarios are depicted in Fig. 5, showcasing the transportation of hydrogen produced at wind farm sites at 30 bar through pipelines directly to the greenhouse.

In all the scenarios, the produced hydrogen is utilized in combined heat and power (CHP) engines—either solely hydrogen-fired or using a hydrogen-natural gas blend—to generate 13.3 MW of electricity. Baseline data from conventional natural gas-fired CHP engines were used to ascertain fuel consumption, total heat and power output. A market-available hydrogen-burned CHP engine model was then selected to determine the heat input and fuel consumption necessary for the same power output. From this, the individual hydrogen demand for each blending ratio was calculated.

For the nine scenarios, the design parameters for the electrolyzer, compressor, tube trailer, and pipeline were computed based on an assumption of 5 and 10 days of hydrogen storage capacity respectively, an operational duration of 1,010 h per year, and the greenhouse operating as a peaking power plant for 6 h daily, equivalent to 2,190 h per year respectively. These power plant operational figures are taken directly from the participating greenhouse partner.

Equipment costs, as well as operation and maintenance expenses,

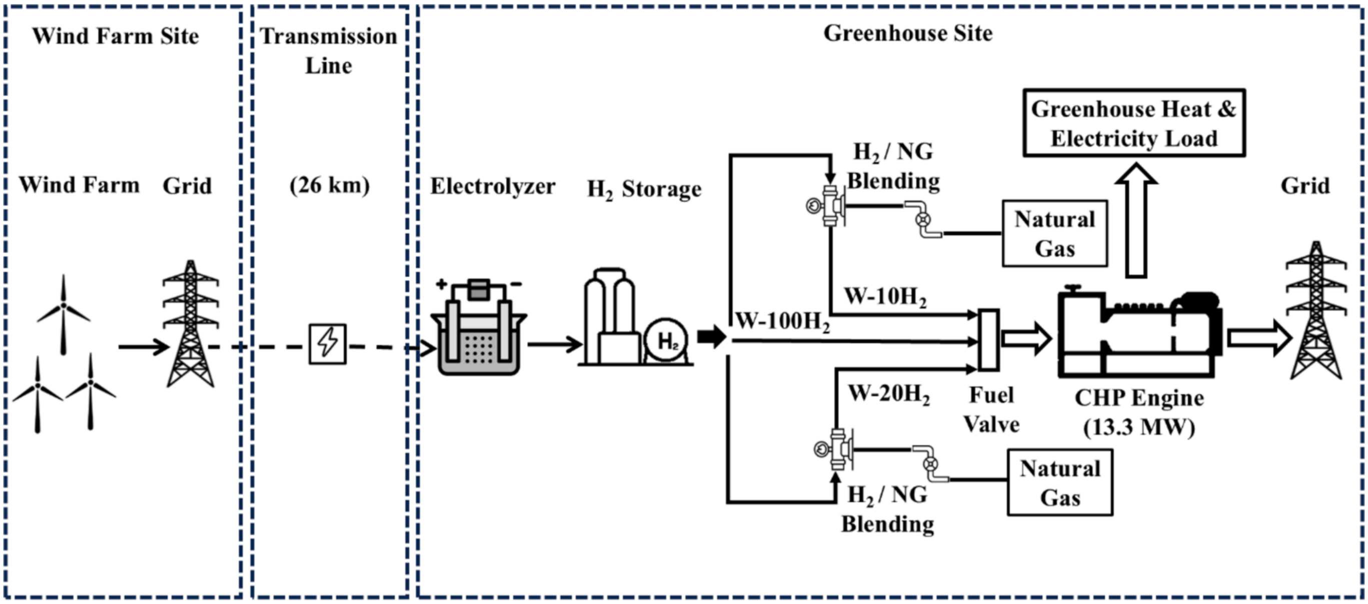

Fig. 3. Case scenarios W-10H_2, W-20H_2, W-100H_2.

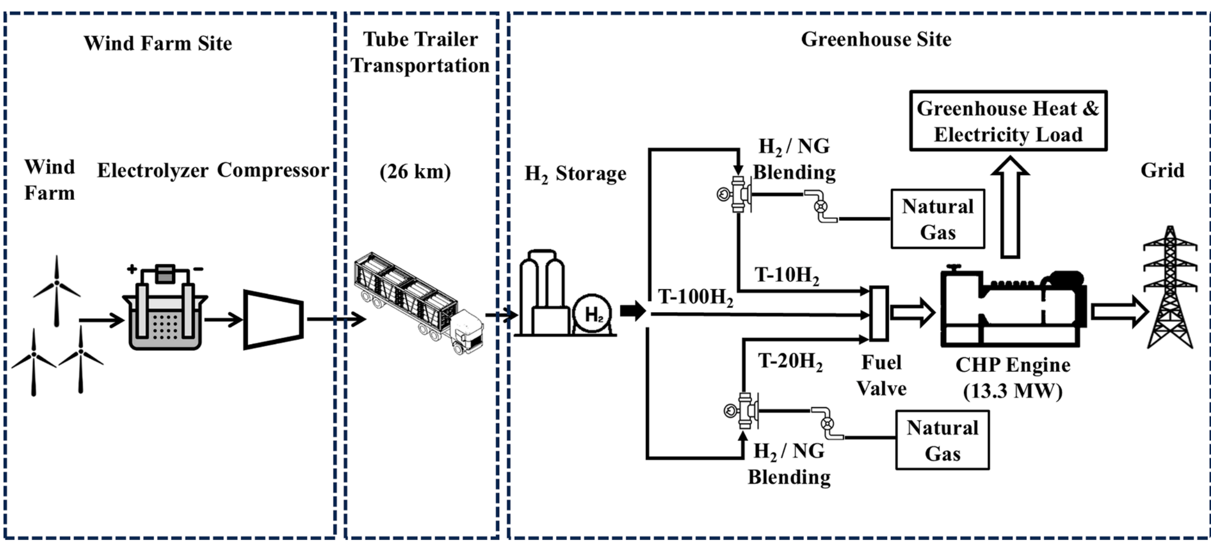

Fig. 4. Case scenarios T-10H_2, T-20H_2, T-100H_2.

were sourced from various recently published literature examples and adjusted to current US dollars, factoring in inflation and exchange rates. A 20-year analysis period and a 6 % discount rate were employed to calculate the levelized cost of hydrogen (LCOH), the payback period (PBT), Internal Rate of Return (IRR), and Discounted Payback Period (DPB).

5. Data collection

Data has been collected from both the wind farm and the greenhouse, including heat and electricity production from CHP engines, as well as associated information such as natural gas consumption, CO_2 emissions, and utilization, which are described in the following sections.

5.1. Greenhouse data

In this case study the data are collected from a Leamington Area Greenhouse, Ontario, Canada. It is 25 acre Bell Pepper Greenhous having average yield of 34 kg of peppers per m^2 [48]. The farming operation also includes 13.3 MW of grid connected generation capacity using four 3.3 MW natural gas fired CHP engines and five 8,830 kW of hot water boilers, and a 6,000 m^3 hot water tank to maintain an ideal temperature in the greenhouse. Fig. 6 illustrates the thermal circuit of the greenhouse where the hot water is taken from the CHP economizer, plate heat exchanger; hot water boiler which contributes to the hot water tank to maintain a certain temperature in the tank. The hot water from the header is supplied to the greenhouse to maintain an ideal temperature with blowers and after releasing heat the cold or warm water will be reverted to feed water tank. On the power side, the electricity is produced at 4,000 V by the CHP engine and stepped up at 28,000 V to export it to grid. When the engines are running, the auxiliary usage and plant usage electricity is taken from engine itself, but when the engines are not running, power are taken from grid using a step-down transformer at 600 V.

Fig. 7 illustrates the monthly summation of electricity production, heat production, electricity usage, and auxiliary consumption within the

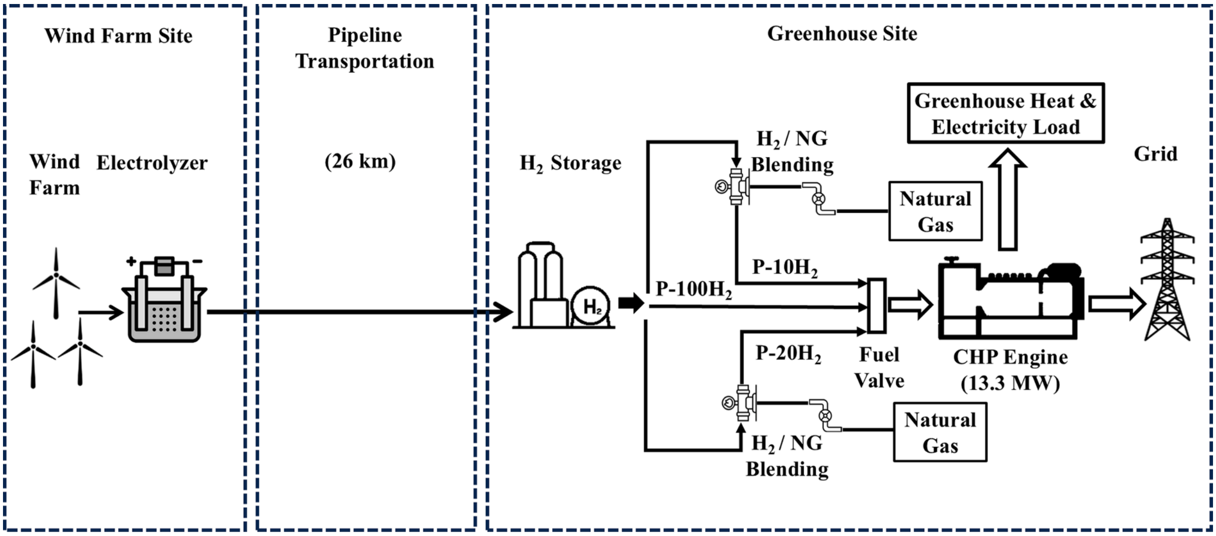

Fig. 5. Case scenarios P-10H_2, P-20H_2, P-100H_2.

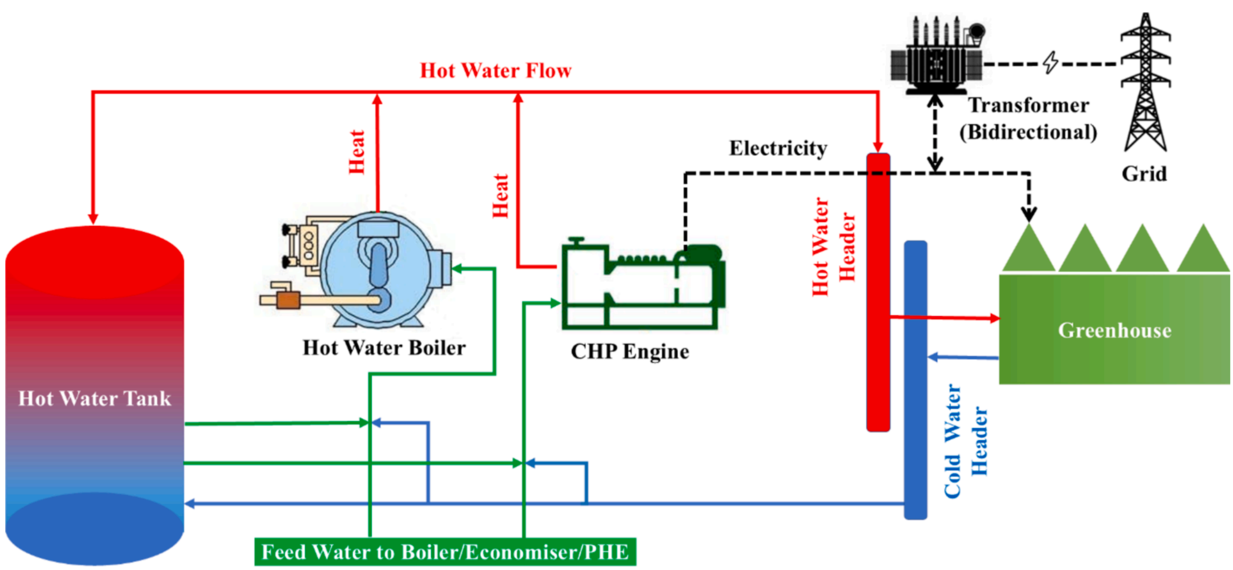

Fig. 6. Heat balance of greenhouse.

greenhouse, as well as the electricity import and export associated with the CHP engines, measured in MWhr/month. This data is derived from hourly recordings taken at the Leamington Area Greenhouse. The electricity import/export figures are calculated by subtracting the total electricity usage and auxiliary consumption from the total electricity production. In the analyzed year, the greenhouse produced a total of 10,336 MWhr, peaking at 14.06 MWhr on December 21st. Heat production has a total of 11,172 MWhr and maximum production of 15.82 MWhr on September 20th. Of this production, 2,094 MWhr was consumed for operational usage, and 187 MWhr was allocated to auxiliary needs, resulting in a net electricity export to the grid of 8,054 MWhr for the year, with an annual operational time of 1,010 h. Notably, the graph indicates that in March, the greenhouse imported 64 MWhr from the grid due to the unavailability of the CHP engines.

Fig. 8 presents the monthly summation of natural gas consumption by the CHP for the analyzed year, which recorded an annual operating time of 1,010 h. The total natural gas consumption amounted to 2.58 million m^3 per year, with a minimum usage of 35,000 m^3 in March, reflecting reduced operation of the CHP engine during that month. The corresponding CO_2 emissions are also depicted, totaling 14,182 tons per year. As the objective is to reduce this huge amount of CO_2 emission, H_2 is blended with natural. If hydrogen is blended with natural gas, significant reductions in CO_2 emissions can be achieved: 539 tons per year for a 10 % hydrogen blend, 1,078 tons per year for a 20 % blend, and 5,390 tons per year for a 100 % hydrogen blend. Table 5 summarizes the CO_2 emission reduction data for these three blending ratios, based on the actual operating time of 1,010 h per year, as well as a theoretical scenario with full power output from all engines totaling 29,127 MWhr per year at 2,190 h.

5.2. Wind farm data

In this paper the wind farm considered is Southwestern Ontario Wind Farm. The total capacity of wind farm is 200 MW having 101.2 MW at Wind Farm Phase 1 and 99.4 MW at Wind Farm Phase 2 [49]. Fig. 9 illustrates the monthly electricity generation data from Wind Farm Phase 1, Phase 2, and the overall electricity supply for the analyzed year. The average power output was 35.13 MW for Phase 1 and 37.98 MW for Phase 2. Notably, August recorded the lowest total electricity supply at 22.40 GWh/month. In the case scenario T-100H_2, the electrolyzer

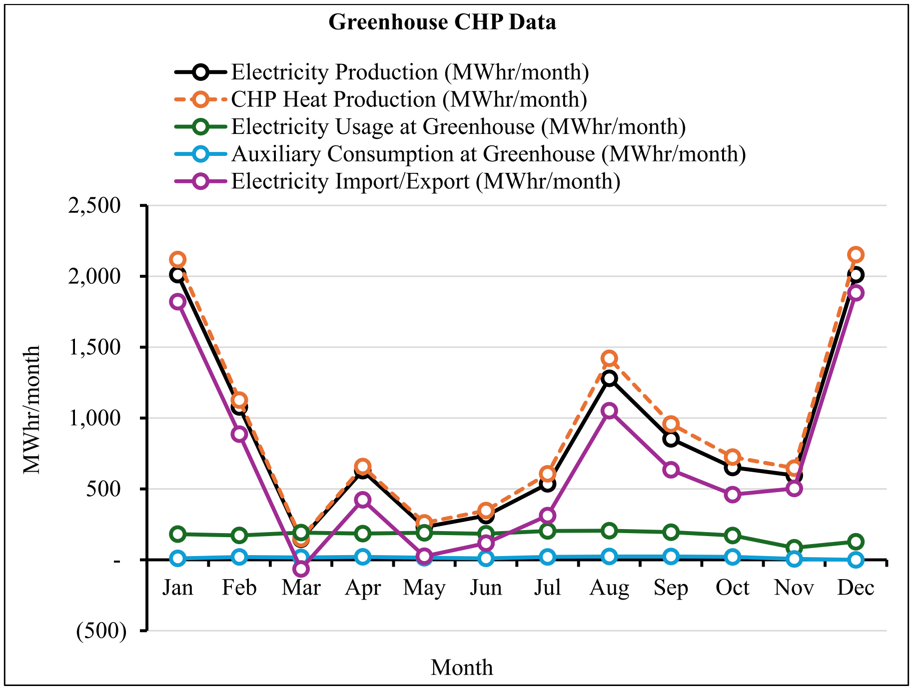

Fig. 7. Greenhouse CHP data.

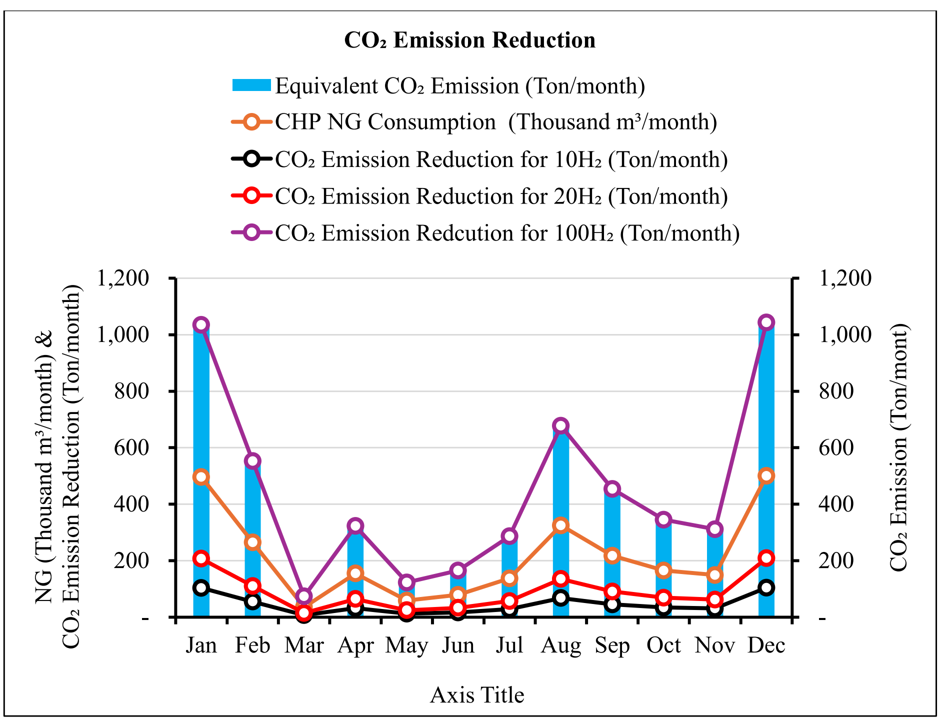

Fig. 8. CO_2 emission reduction from CHP engine at $10H_2$, $20H_2$, $100H_2$.

Table 5
Carbon dioxide emission reduction data.

Annual Operating Hour (hr/yr)	CHP Electricity Output (MWhr/yr)	Equivalent NG Consumption (Million m^3/yr)	Equivalent CO_2 Emission (ton/yr)	CO_2 Emission Reduction at $10H_2$ (ton/yr)	CO_2 Emission Reduction at $20H_2$ (ton/yr)	CO_2 Emission Reduction at $100H_2$ (ton/yr)
2,190	29,127	6.79	14,182	1,418	2,836	14,182
1,010	10,336	2.58	5,390	539	1,078	5,390

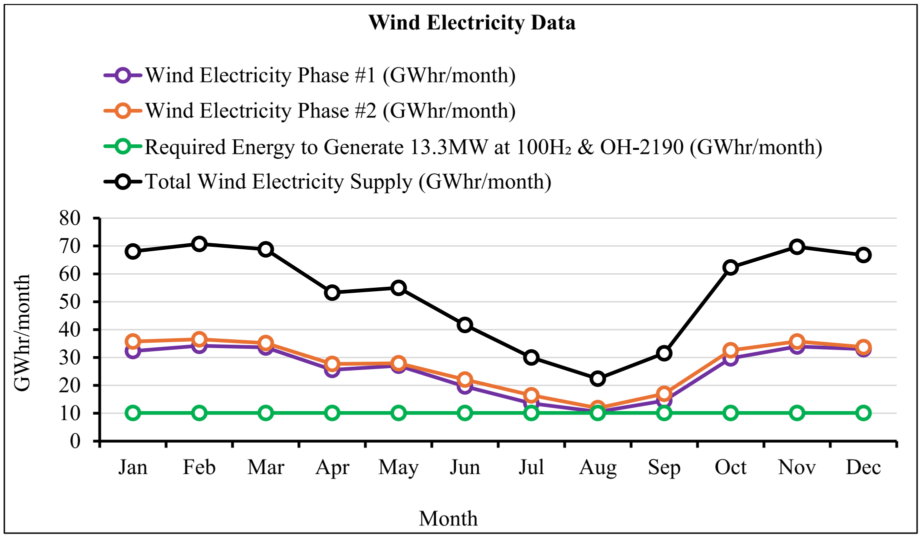

Fig. 9. Wind electricity data.

demands the maximum energy input, utilizing 100 % H_2 to fuel the CHP engine for generating 13.3 MW. Additionally, in this tube trailer scenario, the produced H_2 will be compressed to 500 bar at the wind farm site for transport to the greenhouse, which also entails significant energy consumption. Assuming the CHP operates for 6 h per day throughout the year, this results in a total of 2,190 operating hours annually, representing the maximum operational duration in this study. Considering the energy requirements of both the electrolyzer and the compressor, the T-100H_2 scenario necessitates the highest energy consumption among all nine cases, amounting to 10.12 GWh per month, which remains below the minimum electricity output from the wind farm mentioned above. This indicates that the electricity generated from the wind farm is sufficient to meet the power demands of the T-100H_2 case.

5.3. Existing natural gas fired and proposed hydrogen fired combined heat and power (CHP) engine data

Table 6 shows existing natural gas fired CHP engine data including engine make, model, total electrical output, efficiency, and total heat input to produce 13.3 MW electricity and its corresponding lower calorific value and density of natural gas [48]. The data shows the engine requires 106,187 MJ/hr of heat or 3,097.35 m^3/hr of natural gas to generate 13.3 MW of electricity at 100 % load. The proposed H_2 fired CHP engine has 750 kW of electrical output each [50]. Nearly eighteen engines are required to generate the same 13.3 MW of electricity. This engine requires 120,604.53 MJ/hr of heat or 1,003.92 kg/hr of hydrogen to generate 13.3 MW of electricity considering the density of hydrogen of 0.0899 kg/m^3 [11,12,48,50,51].

Table 6
Existing natural gas fired and proposed hydrogen fired engine data.

Criteria	Unit	Existing NG Fired Engine	Proposed H_2 fired Engine
Make & Model		Jenbacher J620	2G-Agenitor 420
Electrical Output per Engine	kW	3,325	750
Total No of Engine	Nos	4	17.73
Total Electrical Output	kW	13,300	13,300
Thermal Output per Engine	kW	3,131	687
Electrical Efficiency at 100 % Load	%	45.09	39.7
Thermal Efficiency at 100 % Load	%	42.5	40.7
Overall Efficiency at 100 % Load	%	87.7	80.4
Total Heat Input to produce 13.3 MW	MJ/hr	106,187	120,604
Lower Heating Value	MJ/ Nm^3	34.2	10.8
Fuel Consumption at 100 % Load		100 % of NG	100 % of H_2
	m^3/hr	3,097	11,167
	kg/hr	**2,349**	**1,003**

5.4. Hydrogen and natural gas blending data

Fig. 10 and Fig. 11 show the volumetric heat content, gravimetric heat content and density of blended gas according to the addition of H_2 from 0 % to 100 % with natural gas [20]. The heat content is based on the lower calorific value of natural gas and H_2 as 34.2 MJ/m^3 and 10.8 MJ/m^3 respectively [11,12,48,51]. The gravimetric heat content is increased from 10.8 MJ/kg to 120 MJ/kg by increasing the percentage of H_2 from 0 % to 100 %. On the other hand, the density is decreased by increasing H_2 with natural gas.

6. Techno-economic parameters

In this study, a techno-economic analysis has been conducted using several parameters, including the levelized cost of hydrogen (LCOH), payback period (PBT), discounted payback period (DPB), and internal rate of return (IRR), which are described in the subsequent sections.

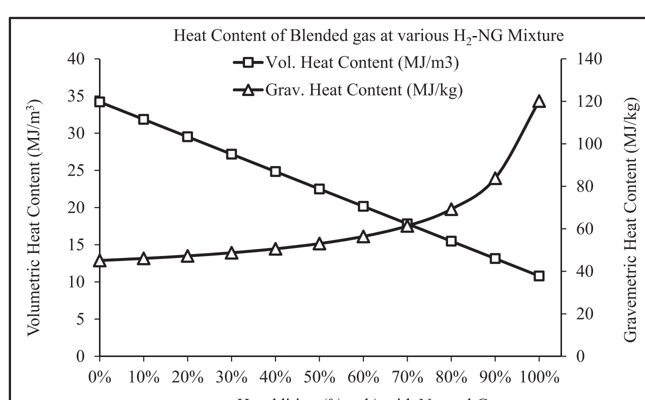

Fig. 10. Heat content of blended gas at various H_2-NG mixture.

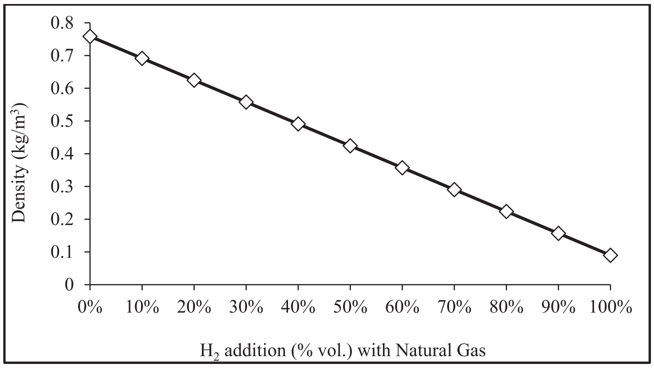

Fig. 11. Density of blended gas at various H_2-NG mixture ratio.

6.1. Levelized cost of hydrogen (LCOH)

LCOH is articulated as the quotient of the total financial outlay Capital Expenditures (CAPEX) plus Operational Expenditures (OPEX) over the aggregate hydrogen output measured in kilograms (M_{H_2}), as detailed in Equation (1) [4]. This calculation involves both the numerator and denominator being tallied annually and then discounted to their present value [4]. For the purpose of this analysis, a projection span of 20 years is employed, aligning with the anticipated lifespan of a wind farm, and a discount rate (r) [28] is set at 6 %.

$$\mathrm{LCOH} = \frac{\sum_{t=0}^{T}\frac{\mathrm{CAPEX}+\mathrm{OPEX}}{(1+r)^t}}{\sum_{t=0}^{T}\frac{M_{H_2}}{(1+r)^t}} \tag{1}$$

The Capital Expenditure (CAPEX), delineated in **Equation (2)**, is the initial investment required for the entirety of the system components at inception, with subsequent years assuming a null value except for instances of technology replacement [28]. Another critical financial aspect considered is the Operational Expenditure (OPEX), delineated in **Equation (3)**. This includes the Operational and Maintenance (O&M) costs for each component, the charges for electricity acquired from the grid, and the profits from electricity supplied back to the grid.

$$\mathrm{CAPEX} = C_{el} + C_{comp} + C_{tank} + C_{pipe} + C_{blend} \tag{2}$$

$$\begin{aligned}\mathrm{OPEX} = {} & O\&M_{el} + O\&M_{stack\ repl} + O\&M_{comp} + O\&M_{tank} + O\&M_{trail} \\ & + O\&M_{pipe} + O\&M_{blend} + C_{water} + C_{insurance} + C_{elec\ pur} - C_{elec\ sel}\end{aligned} \tag{3}$$

6.2. Payback period (PBT)

The PBT is indicative of the time frame required to recoup the initial investment based on the proceeds from selling the hydrogen produced [28]. Payback period is the period of time required to reach the break-even point (the point at which positive cash flows and negative cash flows equal each other, resulting in zero) of an investment based on cash flow [52]. The formula for payback period is in **Equation (4)** [52].

$$\mathrm{PBT} = \frac{C_0}{CF_a} \tag{4}$$

6.3. Discounted payback period (DPB)

The discounted payback period (DPB) accounts for the time value of money by applying the discount rate 'r' to each period's net cash flows before summing them and comparing them with the initial investment. This calculation presumes that the quantity of hydrogen generated, its selling prices, and the operational and maintenance (O&M) expenses for the electrolyzer, compressor, tube trailer, pipeline, storage tank, and blending remain constant annually. This assumption gives rise to the formula presented in **Equation (5)** for calculating the DPB [14].

$$DPB = \frac{ln\left[\frac{1}{1-r\frac{C_0}{CF_a}}\right]}{ln(1+r)} \tag{5}$$

6.4. Internal rate of return (IRR)

Internal rate of return (IRR) is an expression of the highest possible rate of interest that the investment can earn [34]. The IRR is the discount rate that makes the final NPV zero; it can be derived from the following **Equation (6)**:

$$NPV = \sum_{t=0}^{T}\frac{CF_t}{(1+IRR)^t} = 0 \tag{6}$$

7. Annual hydrogen demand calculation for combined heat and power (CHP) engines

Using the data from Table 6, Fig. 10 and Fig. 11, the required blended heat, blended gas consumption and consequently the H_2 consumption for each blending criteria to generate 13.3 MW power from the CHP engines is calculated [20,50], which is shown in Table 7. The table calculates the H_2 consumption for $10H_2$, $20H_2$, and $100H_2$ as 30.37 kg/hr, 66.43, and 1,003.92 kg/hr respectively. Throughout this study the annual operating hours for CHP engines are considered as 2,190 hrs/yr and 1,010 hrs/yr respectively. The annual operating hours (OH) for the CHP engines are set at 2,190 h, based on 6 h of operation per day multiplied by 365 days a year for peaking power plant operations. In contrast, the actual operating hours of the CHP engines at the greenhouse during the analyzed year totaled 1,010 h. These are designated as OH-2190 and OH-1010, respectively. Based on these operating hours, annual H_2 demand is shown in Table 8**.**

8. System/equipment selection

The CAPEX and OPEX encompass various costs, including those associated with the electrolyzer, which is determined by its specific energy consumption; the compressor, also defined by its specific energy consumption; the installation of pipelines with specified diameter sizing; the cost of the tube trailer with its capacity; and along with all associated O&M costs. Therefore, careful selection of the afore-mentioned systems with their capacity or sizing is essential.

8.1. Electrolyzer

There are various electrolysis technologies available and among them Alkaline Electrolyzer (AE), Proton Exchange Membrane (PEM) Electrolyzer and Solid Oxide Electrolyzer (SOE) are the most popular [53]. PEM electrolysis offers higher efficiency and versatility, while SOE provides high thermodynamic efficiency but requires higher temperatures and specialized applications [8]. PEM electrolyzers can rapidly balance the fluctuations in wind energy due to their instant response capability. This enables PEM electrolyzers to reduce energy imbalances and ensure a more stable operation of the system. Conversely, AE electrolyzers have a longer start-up time for the electrolysis process compared to PEM electrolyzers [30]. For these reasons, the most optimal option in this study is considered to be PEM electrolyzer technology [30].

Due to its low energy consumption (50 kWh/kg) [15,30,54,55], compact design, high efficiency, rapid response, high current density, and purity greater than 99.998 %, along with its capability to operate at high pressures (30 bar without a compressor) and the potential for scaling up to meet higher output needs, the Cummins Hylyzer-1000 is

Table 7
H_2 demand for each blending criteria.

LHV (MJ/m^3) H_2 = 10.8 NG = 34.2		LHV of Blended Gas	Heat Required to Generate 13.3 MW (MJ/hr) H_2 = 120,604 NG = 106,187		Total Heat of Blended Gas to Generate 13.3 MW	Total Blended Gas Consumption	NG Flow Rate (90 % of Blended Gas)	H_2 Flow Rate (10 % of Blended Gas)	H_2 Flow Rate
H_2	NG	MJ/m^3	H_2	NG	MJ/hr	m^3/hr	m^3/hr	m^3/hr	kg/hr
$10H_2$ – (10 % H_2 + 90 % NG)									
10 %	90 %	31.86	10 %	90 %	107,628	3,378	3,040	337	**30.37**
1.08	30.78		12,060	95,568					
$20H_2$ – (20 % H_2 + 80 % NG)									
20 %	80 %	29.52	20 %	80 %	109,070	3,694	2,955	738	**66.43**
2.16	27.36		24,120	84,950					
$100H_2$ – (100 % H_2 + 0 % NG)									
100 %	0 %	10.8	100 %	0 %	120,604	11,167	–	11,167	**1,003.92**
10.8	0		120,604	–					

Table 8
Annual H_2 demand for CHP engines.

Blending Criteria	Hourly H_2 Consumption (kg/hr)	Annual H_2 Consumption (kg/yr)	
		OH-2190	OH-1010
10 H_2	30.37	66,510	30,673
20 H_2	66.43	145,481	67,094
100 H_2	1,003.92	2,198,584	1,013,959

considered in this study [54,55]. Further, and perhaps most significantly, the industrial partners are currently utilizing this technology, and they are most likely to adopt it again for future projects.

8.2. Compressor and tube trailer

For case scenarios T-10H_2, T-20H_2, and T-100H_2, compressor is required to pressurize the hydrogen up to 500 bar to transport it via tube trailer to greenhouse area. The cost of compression per kg of hydrogen, and required energy consumption at 6 kWhr/kg [12] of hydrogen at 500 bar of a generalized hydrogen gas compressor is included in Table 9. Composite Tube Trailer (Type IV) is considered having dimension (W-H-L) = (8′-8′-40′), Payload = 1,100 kg, Pressure = 500 bar, pressure vessel capacity = 9 × 30″ dia, loading-3hrs, unloading-1hr [56]. The annual O&M cost of one tube trailer is considered 5 % of Trailer CAPEX based on the assumption of fuel efficiency, average trailer speed, labor, fuel cost, number of trips per year [12].

Table 9
Capital Expenditure (CAPEX) Cost.

CAPEX Costing			
Electrolyzer			**Reference**
Specific Power Consumption of Electrolyzer	kWhr/kg	50	[15,30,54,55]
Cost of Electrolizer	USD/kWe	1,221.98	[1]
Compressor			
Hydrogen Compressor @33 kg/hr and > 500 bar	USD/set	690,474.98	[62]
Electricity Consumption for Compressor at 500 bar	kWhr/kg	6	[12]
Storage Tank			
Cost of Hydrogen Storage System at 35 bar	USD/kg	357.22	[15]
Cost of Hydrogen Storage System at 525 bar	USD/kg	1,219	[15]
Tube Trailer			
Each Tube Trailer Payload Capacity	kg	1,100	[56]
Cost of Composite Tube Trailer	USD/kg	1,368.2	[56]
Each Tube Trailer Cost	USD/each	1,505,020	
Pipeline			
Cost of H_2 Transportation through pipeline	USD/cm/km	34,770.79	[1]
Blending			
Blending Cost	USD	212,000	[15]
Analysis Period and Discount Rate			
Period of Analysis	year	20	[4]
Discount Rate	%	6	[4]

8.3. Pipeline sizing

The optimum diameter of the pipeline should be determined for parameters such as assumed working pressure, length of the pipeline, roughness, etc. [57]. In the analyzed case, the diameter was determined with a function of inlet pressure. The formula for pipeline diameter is based on the General Flow Equation, which is directly stems from the Bernoulli law as showed in **Equation (7)** [57].

$$D = \sqrt[5]{\frac{16\lambda \bullet Z^2 \bullet R^2 \bullet T^2 \bullet L \bullet \dot{m}^2}{\pi^2 \bullet (Z \bullet R \bullet T \bullet (P_1^2 - P_2^2) - 2 \bullet g \bullet P_{av}^2 \bullet \Delta h)}} \quad (7)$$

Calculations were also performed by Kuczynski et al. [57] for pure hydrogen and methane/hydrogen mixtures, and the corresponding graphs are showed in Fig. 12**.** Based on this graph for pure hydrogen transportation at 1,080 kg/hr of flowrate and 30 bar on inlet pressure, the pipeline size is found to be 150 mm.

9. Assumptions and costings consideration in the study

Table 9 and Table 10 show the CAPEX and OPEX cost. All currencies like Euro, GBP, CAD are adjusted considering the inflation and converted to USD at current conversion rate [58–60]. The assumptions are given below:

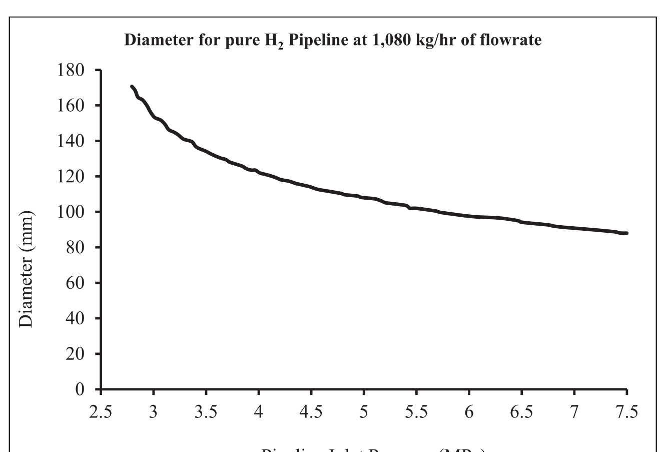

Fig. 12. Diameter for pure hydrogen pipeline as a function of pipeline inlet pressure.

Table 10
Operational Expenditure (OPEX) Cost.

OPEX Costing	Reference			
O&M of Electrolyzer	$O\&M_{el}$	1.5 %	of Ini Inv Cost	[15]
Stack Replacement	$C_{stack\ rep}$	30 %	of Ini Inv Cost	[15]
O&M of Compressor	$O\&M_{comp}$	1.5 %	of Ini Inv Cost	[15]
O&M of Tank	$O\&M_{tank}$	1.5 %	of Ini Inv Cost	[15]
O&M of Trailer	$O\&M_{trail}$	5 %	of Ini Inv Cost	[12]
O&M of Pipeline	$O\&M_{pipe}$	0.00001 %	of CAPEX	[1]
O&M of Blending	$O\&M_{blend}$	1.5 %	of Ini Inv Cost	[15]
Insurance Cost	$C_{insurance}$	0.5 %	of CAPEX	[63]
Electricity Consumption, Purchase and Sell	**Reference**			
Electricity Purchase Rate from grid	USD/MWhr	58.83	[61]	
Annual Electricity generation from CHP Engine	MWhr/yr	29,127	As per OH	
Auxiliary Consumption of CHP Engine	MWhr/yr	55.39	[48]	
Electricity Usage at Under Sun Acres	MWhr/yr	2,153.2	[48]	
Electricity Selling Rate to Grid	USD/MWhr	32.4	[48]	
DM Water				
DM Water Requirement	L/kg of H_2	9	[15,54,55]	
Gross Water Cost	USD/m3	1.86	[15]	

9.1. Assumptions

- The annual operating hours (OH) for the CHP engines are set at 2,190 h per year and 1,010 h per year, respectively, based on the assumption that the CHP operates for 6 h per day over 365 days, as well as the actual operating hours recorded in the analyzed year. Comparing both theoretical and actual operating hour data will provide valuable insights for assessing the feasibility of the nine cases in terms of LCOH, IRR, PBT, and DPB. Operating hours are crucial parameters, as they significantly influence both capital CAPEX and OPEX cost, along with the annual cash flow.
- The storage capacity is defined as the number of days required to accommodate varying consumption rates at different blending ratios and annual operating hours, as represented by **Equation** (8).

$$\text{Storage Capacity (kg)} = \frac{\frac{\text{kg}}{\text{hr}} \times \text{OH}\left(\frac{\text{hrs}}{\text{yr}}\right)}{\frac{365\text{ days}}{\text{yr}}} \times \text{no. of days} \tag{8}$$

- In this study, options for 5 days and 10 days of storage have been considered, reflecting the diverse hydrogen consumption patterns at various blending ratios and transportation modes. This approach ensures that greenhouse operations remain uninterrupted, providing sufficient backup hydrogen during full-load conditions of the CHP engines.

- Annual electricity purchase from wind power connected grid is determined from the power consumed by electrolyzer and H_2 compressor as per the following **Equation** (9).

$$AnnualElectricityPurchaseFromGridorWindPower\left(\frac{USD}{yr}\right) = \{(ElectrolyzerConsumption + H_2CompressorConsumption)\}\left(\frac{MWhr}{yr}\right) \times ElectricityPurchaseRate\left(\frac{USD}{MWhr}\right) \tag{9}$$

- Annual electricity sold to grid is determined by subtracting the CHP auxiliary consumption from total annual electricity generation from CHP engine based on operating hour of 2190 and 1010 hr/yr respectively as per the following **Equation** (10).

$$\text{Annual Electricity Sold to Grid from CHP Engine}\left(\frac{\text{USD}}{\text{yr}}\right) = \left[\left\{13.3\,\text{MW} \times \text{Annual Operating Hour (OH)}\left(\frac{\text{hr}}{\text{yr}}\right)\right\} - \left\{(\text{Auxiliary Consumption at Greenhouse} + \text{Electricity Usage at Greenhouse})\left(\frac{\text{MWhr}}{\text{yr}}\right)\right\} \times \text{Electricity Selling Rate}\left(\frac{\text{USD}}{\text{MWhr}}\right)\right] \tag{10}$$

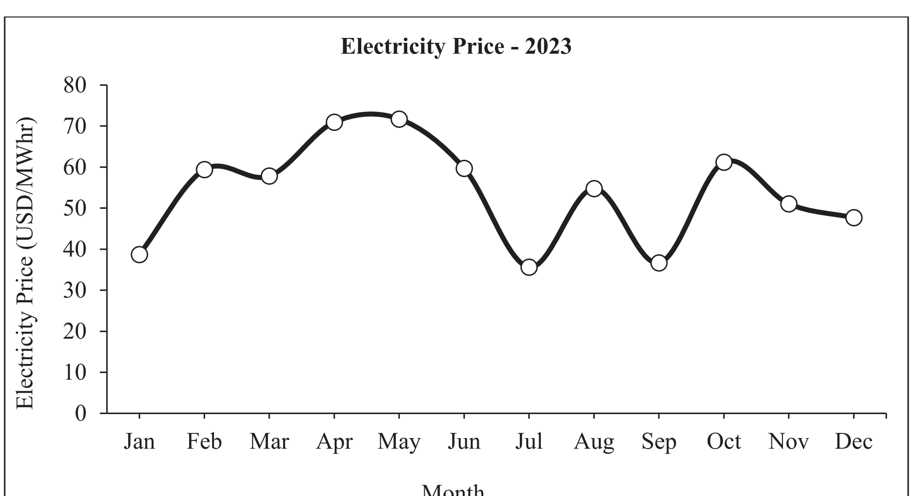

Fig. 13. Electricity price in 2023.

- The payback period, discounted payback period, and internal rate of return are calculated based on the annual cash flow, assuming the system is configured to sell hydrogen to a general market at a price of USD 5.30 per kilogram [15,28].

9.2. Electricity Price

Electricity purchase price is taken from Independent Electricity System Operator (IESO) website [61]. Fig. 13 shows the rate in 2023, where the maximum was USD 71.13/MWhr in May and minimum was USD 35.63/MWhr in July. Whereas in 2024 the price was USD 33.03, USD 47.75, and USD 58.83 per MWhr in Jan, Feb and Mar respectively. In this study the electricity purchasing price from grid is taken as the price in Mar-2024 which is 58.83 USD/MWhr. On the other hand the electricity selling price to the grid is taken as USD 32.40/MWhr [48]. All the prices are adjusted considering the inflation and converted to the current USD rate.

10. Results and discussions

Fig. 14 and Fig. 15 show CAPEX costs and annual electricity consumption of all the nine cases at OH-2190, OH-1010 and Storage-10, 5 days respectively. T-100H$_2$ at OH-1010 Storage-10 days has the maximum cost (USD 146 million), and W-10H$_2$ at OH-2190 and Storage-5 days has a minimum cost of (USD 2.4 million). The capital expenditure (CAPEX) is largely attributed to the substantial costs associated with hydrogen production at the T-100H$_2$ facility, which relies on electrolyzers with an electricity consumption rate of 50 kWh/kg. This includes costs related to the tube trailer and the compression of hydrogen up to 500 bar, as well as the significant expenses for the storage tanks required for T-100H$_2$ blending. Conversely, the W-10H$_2$ scenario incurs no

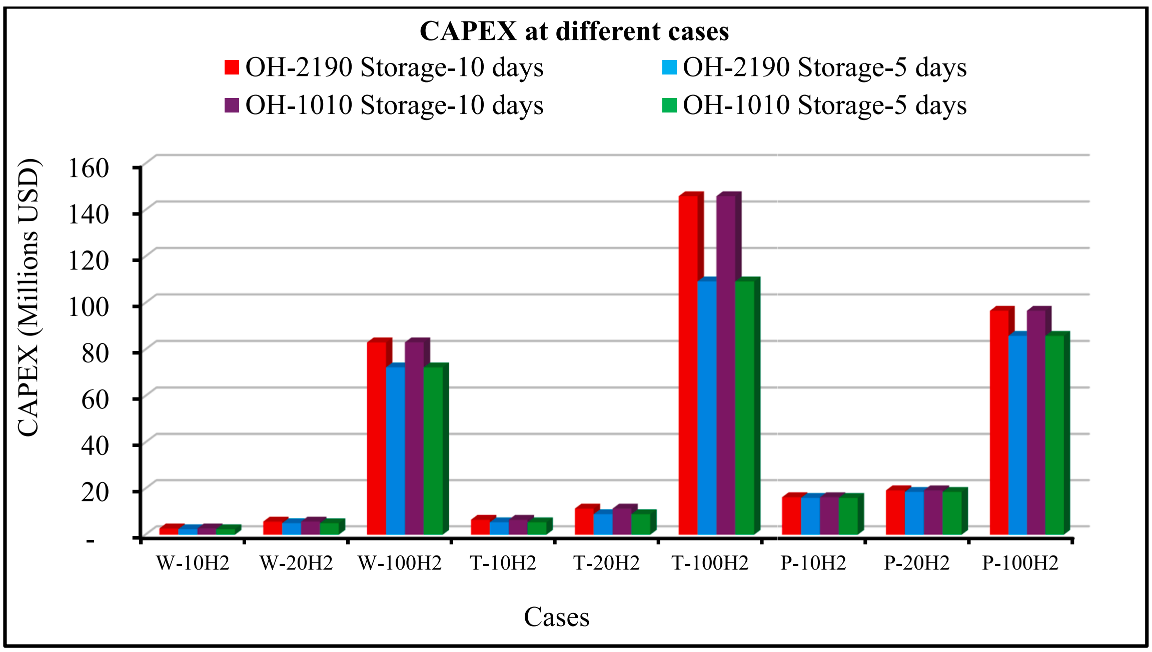

Fig. 14. CAPEX at different OH and storage capacity.

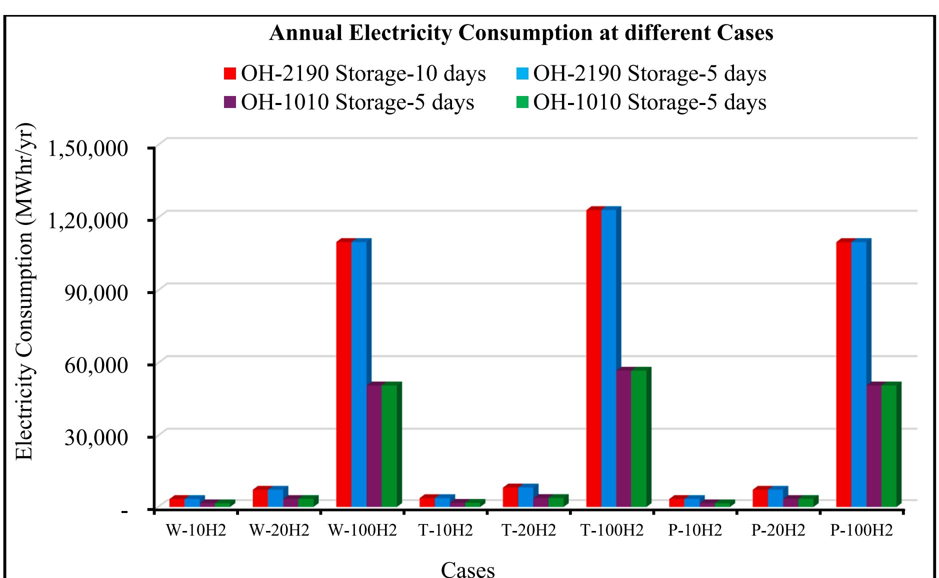

Fig. 15. Annual electricity consumption at different OH and storage capacity.

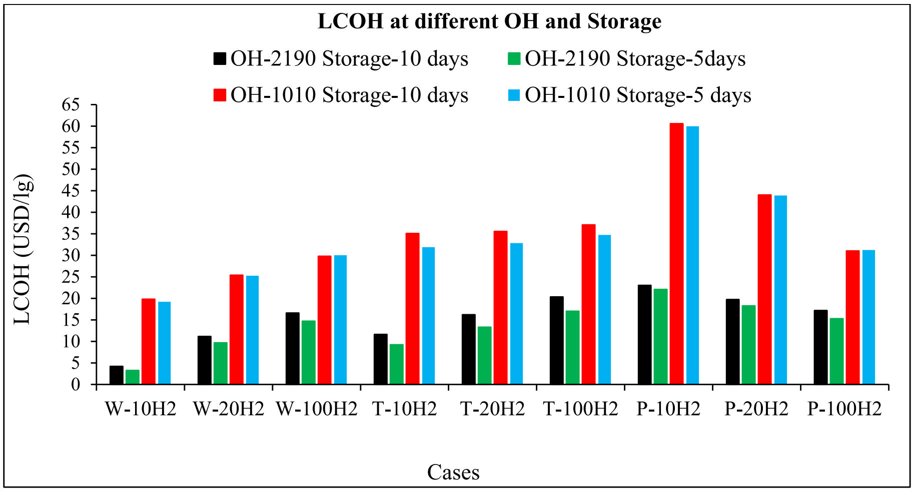

Fig. 16. LCOH (USD/kg) for all cases.

compressor costs and features lower expenses for hydrogen production at the $10H_2$ blending ratio, along with a comparatively smaller storage tank.

When examining electricity consumption, the T-$100H_2$ scenario with an operating hour of 2,190 and a storage capacity of 10 days exhibits the highest energy consumption, totaling 123,120 MWh/year. This elevated demand is primarily due to the additional power required for producing and compressing of hydrogen at $100H_2$ blending criteria, which necessitates 50 kWhr/kg and 6 kWh/kg of energy to achieve a compression level of 500 bar respectively. In contrast, the P-102 scenario operating at 1,010 h and a storage capacity of 10 days demonstrates the lowest energy consumption, amounting to 1,534 MWh/year. This is attributable to the absence of power requirements for compression, alongside reduced hydrogen production costs at the $10H_2$ blending ratio. These findings underscore the significant power consumption associated with the compressor, essential for hydrogen transportation via tube trailer. Overall, the blending ratio and transportation mode are critical factors that influence both CAPEX costs and electricity consumption.

Fig. 16 illustrates the Levelized Cost of Hydrogen (LCOH) at OH-2190 for nine cases with 1, 010, and 10 & 5 days of storage capacity. The W-$10H_2$ case at OH-2190 with 5 days of storage exhibits the lowest LCOH at USD 3.69/kg, while W-$10H_2$ at OH-2190 with 10 days of storage has an LCOH of USD 4.22/kg. Here, storage duration and operating hours significantly impacts the LCOH. Conversely, P-$10H_2$ at OH-1010 with 10 days of storage records the highest LCOH at USD 60.58/kg. The pipeline installation cost remains the same for both scenarios at OH-1010, irrespective of the 5 or 10 days of storage, since P-$10H_2$ produces significantly less hydrogen compared to P-$100H_2$. Consequently, P-$100H_2$ demonstrates a lower LCOH than both P-$10H_2$ and P-$20H_2$. For T-$10H_2$, T-$20H_2$, and T-$100H_2$, the LCOH values at OH-1010 for both 10 and 5 days of storage are nearly identical due to the tube trailer and compression costs varying with the blending ratio. Ultimately, the blending ratio emerges as a crucial factor influencing the LCOH, along with the transportation mode either tube trailer or pipeline installation, which also significantly affects costs.

Among the wired, tube trailer, and pipeline categories, the Levelized Cost of Hydrogen (LCOH) is lowest for the wired option based on their respective blending criteria. More specifically, among the W-$10H_2$, W-$20H_2$, and W-$100H_2$ options, W-$10H_2$ exhibits the lowest LCOH at OH-2190 with 5 days of storage. Fig. 17 illustrates the variations in net present value (NPV) for capital expenditures (CAPEX), operational expenditures (OPEX), and hydrogen production, clearly demonstrating a significant increase in OPEX for 100 % hydrogen blending due to the substantial electricity consumption required for electrolysis each year.

Fig. 18 displays the payback period (PBT) for all nine cases. The results indicate that W-$100H_2$ at OH-2190 with 5 days of storage has the shortest payback period of 6.205 years, attributed to its maximum annual operating hours and suitable storage capacity. Both operating hours and storage capacity significantly influence annual cash flow and initial investment costs. In contrast, P-$10H_2$ at OH-1010 with 10 days of storage exhibits the longest payback period of 100.14 years, suggesting it is not feasible based on this metric, primarily due to the substantial initial investment required for pipeline installation relative to the lower cash flow from the $10H_2$ blending ratio. The shorter PBT for P-$100H_2$ is a result of its high hydrogen demand. Among the tube trailer cases, T-$100H_2$ has a lower PBT compared to T-$10H_2$ and T-$20H_2$, highlighting the critical role of annual cash flow driven by high hydrogen demand. Overall, W-$100H_2$ incurs the lowest initial investment while generating the highest annual cash flow.

Fig. 19 illustrates the internal rate of return (IRR) for various scenarios. The W-$100H_2$ case at OH-2190 with a 5-day storage duration exhibits the highest IRR at 15.16 %. However, as indicated in the figure, most scenarios present negative IRR values, suggesting they are not viable options. This implies that the cash inflows are insufficient to cover the initial investment and associated costs over time, considering a discount rate of 6 %. Specifically, cases such as T-$10H_2$, T-$20H_2$, T-$100H_2$, P-$10H_2$, and P-$20H_2$ show significantly negative IRR values, primarily due to extremely high initial investment costs paired with very low cash inflows. These negative values further indicate that these cases are not financially viable options in terms of IRR.

Fig. 20 presents the discounted payback period (DPB) for all nine cases across various operating hours and storage durations. Cases that reach the maximum horizontal line indicate infeasibility, meaning the investments in these scenarios will never be recouped at a discount rate of 6 %. The W-$100H_2$ case at OH-2190 with a 5-day storage duration shows the minimum DPB of 7.993 years, highlighting that increased operating hours, reduced storage duration, and maximum hydrogen blending are key factors for achieving a lower discounted payback period. Notably, each case has at least one infeasible option. For instance, even in the W-$100H_2$ scenario, a case of 1010 operating hours with 10 days of storage results in an extremely high DPB, indicating that the investment will never be recovered. Additionally, in the cases of P-$10H_2$ and P-$20H_2$, all four options were deemed infeasible due to their excessively high investments relative to low cash inflows.

Table 11 shows the most feasible option in terms of all parameters. The table clearly indicates that that more operating hour of CHP engine, maximum H_2 production with lower storage capacity and avoiding transportation of hydrogen in such a shorter distance like 26 km are the key factors to get a feasible option like W-$100H_2$.

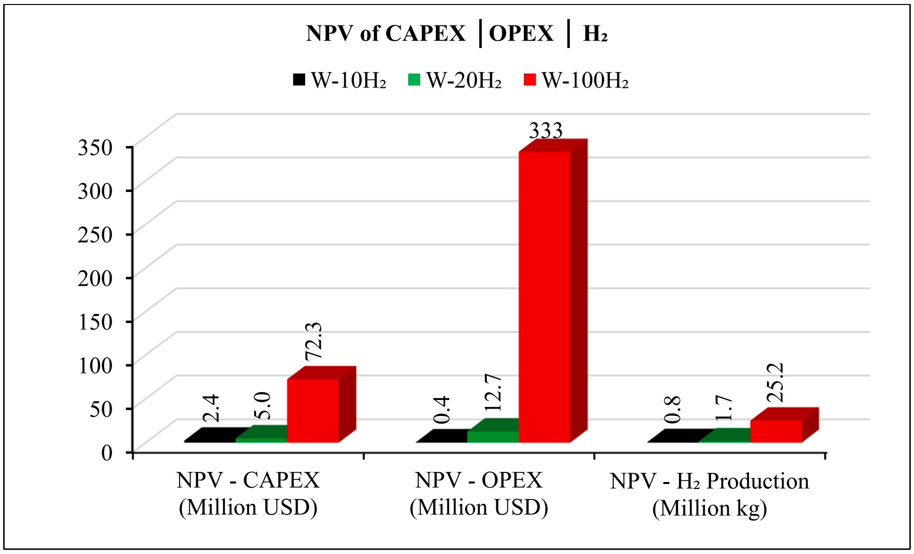

Fig. 17. Variation of NPV of CAPEX, OPEX and H_2.

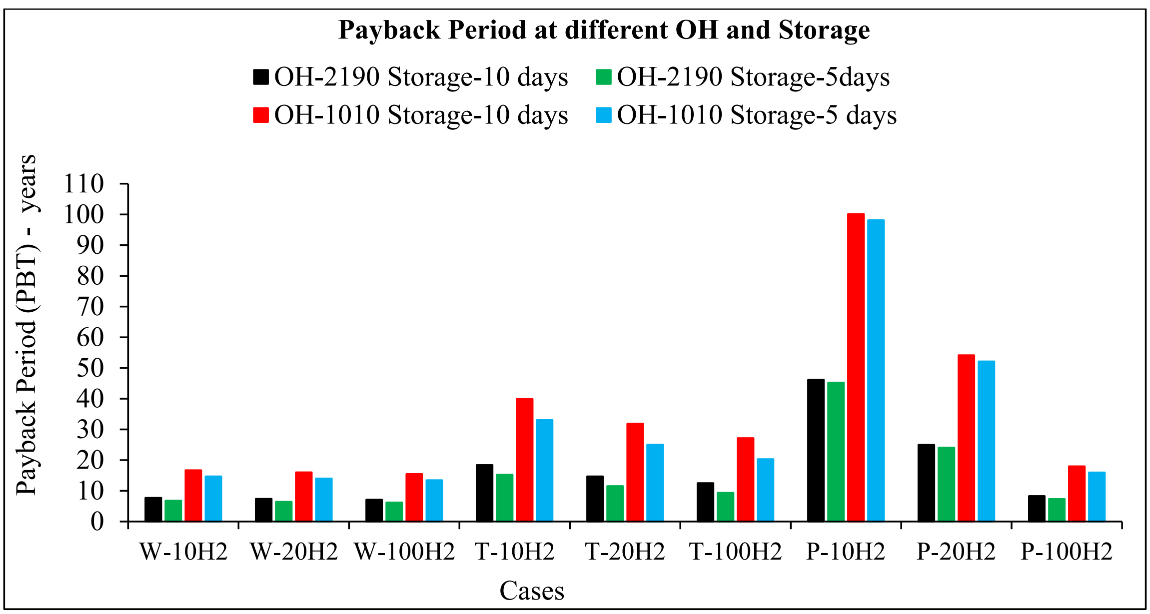

Fig. 18. Payback Period (PBT) for all nine cases.

11. Sensitivity analysis

Table 12 shows the assumption for the variables in the sensitivity analysis. The Levelized Cost of Hydrogen (LCOH) is primarily influenced by the values of capital expenditure (CAPEX), operational expenditure (OPEX), and annual hydrogen production, as dictated by the relevant equation. Annual hydrogen production is contingent upon the operating hours of the Combined Heat and Power (CHP) engines, which vary according to different blending ratios. Thus, the operating hours of CHP engines are crucial for determining the LCOH. Additionally, the storage capacity for hydrogen, linked to the operating hours, represents another significant CAPEX component. Furthermore, electricity consumption for electrolysis and hydrogen compression, particularly for Tube Trailer cases, is a critical factor. The discount rate also substantially affects the calculation of net present value. Consequently, operating hours, storage capacity, electricity pricing, and the discount rate are identified as having the most substantial impact on LCOH.

The Storage Capacity is considered as the number of days. The range of days from 1 day to 10 days were considered based on the different H_2 configuration variations, i.e. the different blending ratios and transportation modes we studied for hydrogen-based greenhouse operation. In our analysed year, the annual operating hour is 1,010 hrs and for the CHP operation at 6 hrs per day and 365 days per year which is maximum value. This is why we select the range of operating hours from 1,000 hrs to 2,200 h to evaluate the sensitivity of LCOH with the variation of operating hour. For the electricity purchase price, we have relied on the global adjustment (GA) price from IESO [61] which has a very wide range of price from USD 33/MWhr to USD 71/MWhr from January 2023 to March 2024 respectively. As this electricity price can see very wide fluctuation through instant spikes and dips, we have ranged the price from USD 10 to 100 per MWhr to assess the most favourable and worst-case scenarios. For discount rate variation, the literature has largely considered ranges from 5 % to 10 % [4,16]. For our study we have ranged from 2 % to 20 % to see the effect on LCOH considering the 20 % discount rate as worst case scenario.

Fig. 21 shows the LCOH sensitivity on storage in days at OH-2190.

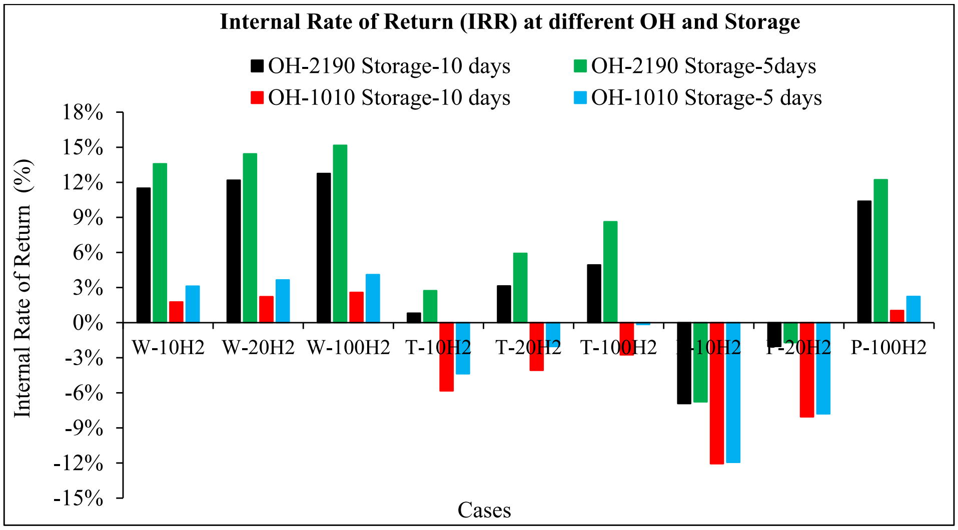

Fig. 19. Internal Rate of Return (IRR) for all nine cases.

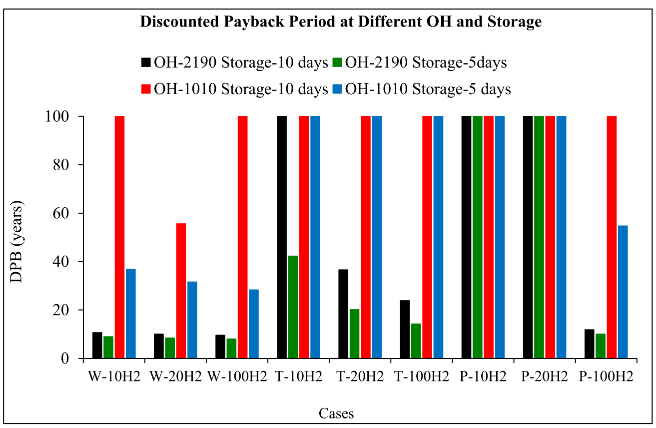

Fig. 20. Discounted payback period at different cases.

Table 11
Most feasible option.

Parameters	Most Feasible Option	Value
Levelized Cost of Hydrogen (LCOH)	W-10H_2 | OH-2190 |5-day storage	USD 3.69/kg
Payback Period (PBT)	W-100H_2 | OH-2190 |5-day storage	6.205 years
Discounted Payback Period (DPB)	W-100H_2 | OH-2190 |5-day storage	7.993 years
Internal Rate of Return (IRR)	W-100H_2 | OH-2190 |5-day storage	15.16 %

The result shows that the case W-10H_2 at the storage capacity of one day has the LCOH of USD 3.27/kg which is the lowest value. On the other hand, the case P-10H_2 has the maximum LCOH which is USD 23.01/kg. It indicates that the storage capacity is an important parameter to increase the CAPEX cost which ultimately increases the LCOH. For all the cases LCOH is increasing with the increase of storage period or storage capacity.

Fig. 22 shows the LCOH (USD/kg) Sensitivity on Annual Operating Hour at 10 days of storage capacity. W-10H_2 at OH-2200 has the LCOH of USD 4.15/kg which is minimum and P-10H_2 at OH-1000 has the highest LCOH which is USD 61.80/kg. It indicates that the higher the operating hour of CHP engines, the higher the requirement of H_2, and the higher the annual hydrogen production to minimize the LCOH. For all the cases LCOH decreased by increasing the operating hour of CHP engines.

Fig. 23 illustrates the sensitivity of levelized cost of hydrogen (LCOH) (USD/kg) to electricity prices at OH-2190 with a 10-day storage duration. The W-10H_2 scenario exhibits the lowest LCOH at an electricity price of USD 10/MWh, while the P-10H_2 scenario has the highest LCOH at USD 25.07/kg when the electricity price reaches USD 100/MWh. This indicates that electricity pricing plays a crucial role in determining LCOH, as a substantial amount of electricity is consumed by the electrolyzer and compressor, sourced from the wind farm, which significantly contributes to overall electricity purchase costs. Additionally, the selling rate for exported electricity from the combined heat and power (CHP) engine at the greenhouse is considerably lower than the purchase rate, according to data from our industrial partner. These factors collectively impact the LCOH significantly.

Fig. 24 shows the LCOH (USD/kg) Sensitivity on Discount Rate at OH-2190 and Storage-10 days. The W-10H_2 case at 2 % discount rate has lowest value of LCOH (USD 3.15/kg). On the other hand, P-10H_2 at 20 % discount rate has the maximum LCOH (USD 51.93/kg). As a higher discount rate reduces the present value of future cash inflows from hydrogen production, making them less valuable in today's terms, the future revenues are discounted more heavily, which can lead to a higher overall cost of hydrogen since the profitability of the project is diminished. That's why it clearly indicates that the higher the discount rate, the higher the LCOH.****

12. Conclusion

- Study of the integration of green hydrogen technology into a commercial greenhouse in Ontario, Canada, revealed that green hydrogen as a replacement for natural gas in CHP engines showed promise as a potentially feasible solution.

Table 12
Assumption for the variables in the sensitivity analysis.

Variables	Minimum Value	Maximum Value	Units
H_2 storage capacity in terms of days	1	10	days
Annual operating hour (OH)	1,000	2,200	hr/yr
Electricity Price	10	100	USD/MWhr
Discount Rate	2 %	20 %	%

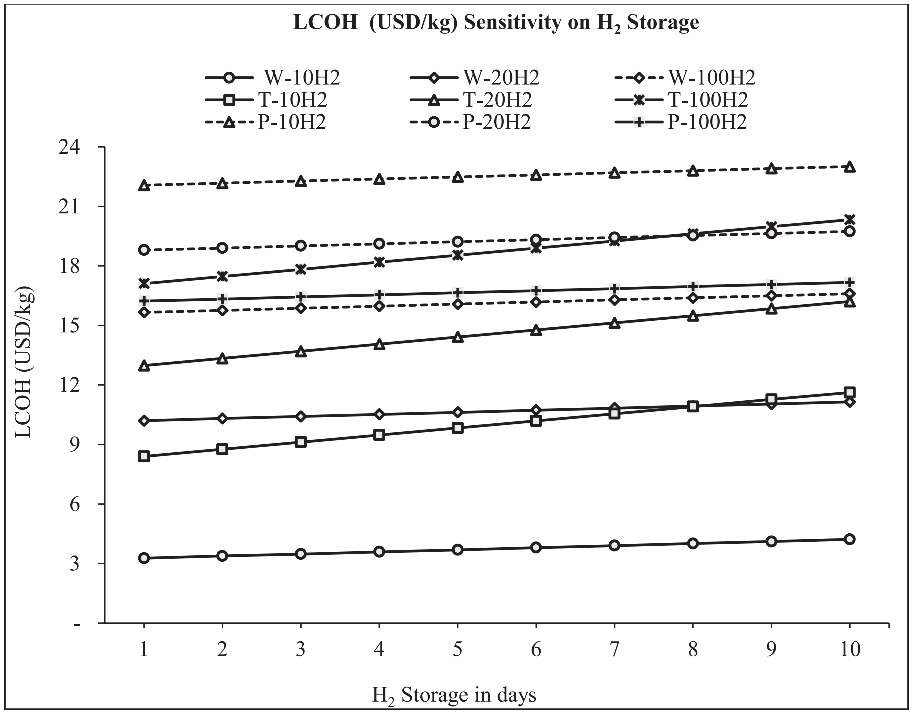

Fig. 21. LCOH sensitivity on H_2 storage.

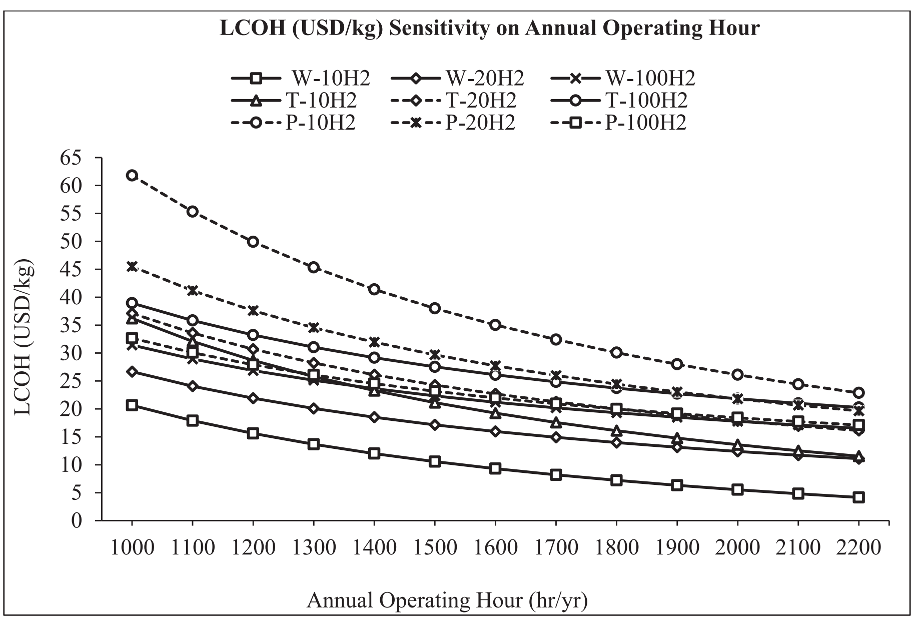

Fig. 22. LCOH (USD/kg) sensitivity on annual operating hour.

- The study evaluated nine different scenarios and found that Scenario W-10H_2 with a 5-day storage capacity and OH-2190 was the most viable option in terms of LCOH at USD 3.69/kg. But in terms of PBT, IRR, and DPB, W-100H_2 with OH-2190 and 5 days storage capacity was the most attractive with values of 6.205 years, 15.16 % and 7.993 years respectively. Conversely, new pipeline installation or transportation via tube trailer over a distance of 26 km is not a feasible option according to the results.
- The findings of our study indicate that while W-10H_2 presents the lowest LCOH, W-100H_2 shows superior financial performance metrics. This discrepancy highlights a crucial trade-off: the lowest cost does not always align with the best financial returns. In the long term, the study suggests that operators need to evaluate their specific circumstances, including operational scale, market conditions, and investment strategies.
- Various studies in the literature review showed that the mixture of volumetric composition up to 20 % hydrogen and 80 % natural gas could be utilized with existing infrastructure without any vital modification. Whereas 100 % H_2 requires some new infrastructure. Consequently, while W-10H_2 may minimize initial costs, the enhanced PBT and IRR of W-100H_2 could yield greater long-term profitability and financial resilience, particularly in markets anticipating rising hydrogen prices.

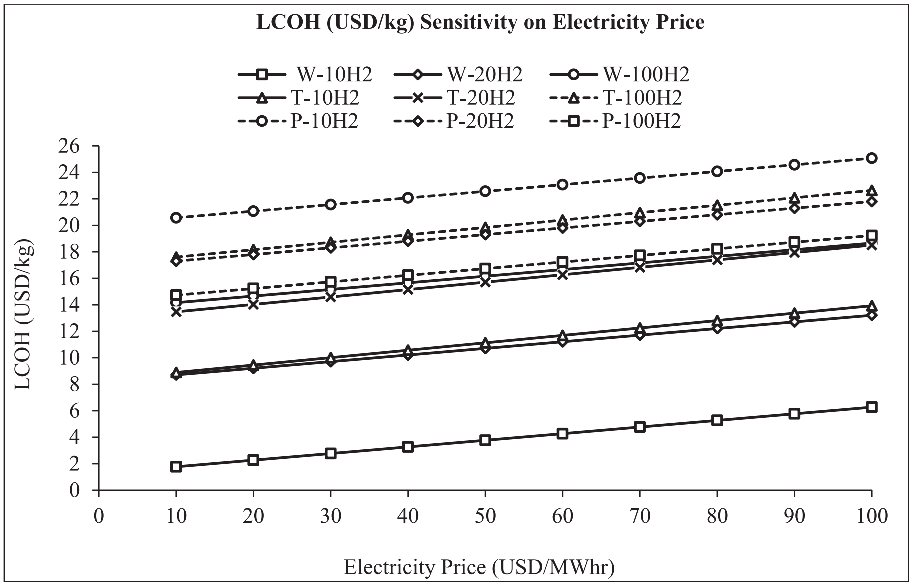

Fig. 23. LCOH (USD/kg) sensitivity on electricity price.

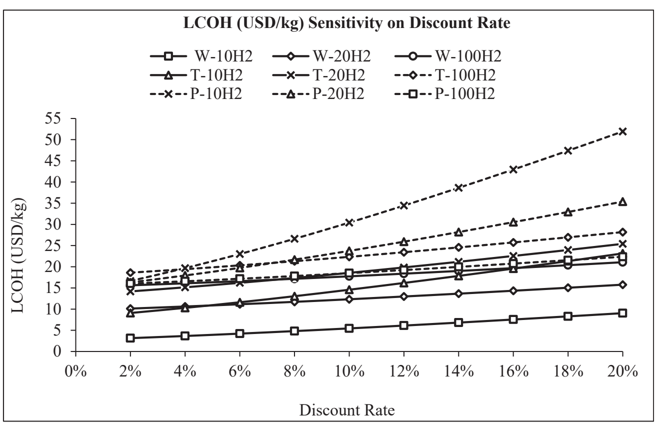

Fig. 24. LCOH (USD/kg) sensitivity on discount rate.

- Operators must consider whether minimizing hydrogen costs (W-10H$_2$) aligns with their long-term financial goals. If initial investments are prioritized, a higher blend ratio (like W-100H$_2$) may yield better returns over time. Understanding how hydrogen prices evolve in their specific market can help operators make informed decisions about which blend to adopt. A market shift towards higher hydrogen prices could make the financial benefits of higher blend ratios more pronounced.
- Depending on their financial capacity and risk appetite, operators might prefer to invest in a blend that offers quicker returns (W-100H$_2$) while still maintaining a focus on sustainable practices. So, the decision on hydrogen blend ratios should consider both cost implications and long-term financial performance, allowing greenhouse operators to optimize their operational strategies accordingly. Overall, this research provides valuable insights into the feasibility of adopting green hydrogen technology for enhanced energy sustainability in the context of commercial greenhouse food production.

13. Future recommendation

1. O_2 output determination from electrolysis byproduct should be considered as it will significantly affect all techno-economic parameters like LCOH and PBT while O_2 selling will then be considered.
2. The storage capacity should be optimized according to the real time wind power supply, real time energy requirement of greenhouse, and the power production from CHP engines based on optimum blending ratio. Because it plays a vital impact on CAPEX cost to determine LCOH and PBT.
3. Considering the distance of 26 km, installation of new pipeline or tube trailer transportation cost will be very high. Having the high value of CAPEX or initial investment cost, the techno-economic parameters show impractical results. In this case H_2 liquefaction and Liquid H_2 tank transportation could be explored for future commercialization. Innovations in high-density storage technologies, such as advanced composite materials or cryogenic storage systems, could increase the capacity and safety of hydrogen storage, making it more practical for widespread use.

CRediT authorship contribution statement

Kayes Md Abu Reza: Writing – original draft, Visualization, Methodology, Investigation, Formal analysis, Data curation, Conceptualization. **David S-K Ting:** Writing – review & editing, Supervision, Resources, Project administration, Funding acquisition. **Rupp Carriveau:** Writing – review & editing, Supervision, Resources, Project administration, Funding acquisition.

Declaration of competing interest

The authors declare that they have no known competing financial interests or personal relationships that could have appeared to influence the work reported in this paper.

Data availability

The data that has been used is confidential.

References

[1] Franco BA, Baptista P, Neto RC, Ganilha S. Assessment of offloading pathways for wind-powered offshore hydrogen production: Energy and economic analysis. Appl Energy 2021;286:116553. https://doi.org/10.1016/j.apenergy.2021.116553.
[2] Costa M, Maka R, Marra FS, Palombo A, Prati MV. Assessing techno-economic feasibility of cogeneration and power to hydrogen plants: A novel dynamic simulation model. Energy Rep 2023;10:1739–52. https://doi.org/10.1016/j.egyr.2023.08.013.

[3] CO2 Emissions in 2023 – Analysis. IEA n.d. https://www.iea.org/reports/co2-emissions-in-2023 (accessed May 7, 2024).
[4] Superchi F, Papi F, Mannelli A, Balduzzi F, Ferro FM, Bianchini A. Development of a reliable simulation framework for techno-economic analyses on green hydrogen production from wind farms using alkaline electrolyzers. Renew Energy 2023;207:731–42. https://doi.org/10.1016/j.renene.2023.03.077.
[5] Marouani I, Guesmi T, Alshammari BM, Alqunun K, Alzamil A, Alturki M, et al. Integration of renewable-energy-based green hydrogen into the energy future. Processes 2023;11:2685. https://doi.org/10.3390/pr11092685.
[6] Hydrogen colours codes - H2 Bulletin n.d. https://h2bulletin.com/knowledge/hydrogen-colours-codes/ (accessed July 3, 2024).
[7] The white gold rush and the pursuit of natural hydrogen. Rystad Energy n.d. https://www.rystadenergy.com/news/white-gold-rush-pursuit-natural-hydrogen (accessed July 3, 2024).
[8] Hassan Q, Algburi S, Sameen AZ, Salman HM, Jaszczur M. Green hydrogen: A pathway to a sustainable energy future. Int J Hydrogen Energy 2024;50:310–33. https://doi.org/10.1016/j.ijhydene.2023.08.321.
[9] Hydrogen Storage. EnergyGov n.d. https://www.energy.gov/eere/fuelcells/hydrogen-storage (accessed March 23, 2024).
[10] Entry EB. HYDROGEN. Thermopedia, Begel House Inc.; 2011. doi: 10.1615/AtoZ.h.hydrogen.
[11] Universal Industrial Gases, Inc. ... Hydrogen Unit Conversion (gas, liquid) n.d. https://www.uigi.com/h2_conv.html (accessed March 23, 2024).
[12] Hydrogen transport and storage cost. GOVUK n.d. https://www.gov.uk/government/publications/hydrogen-transport-and-storage-cost (accessed April 19, 2024).
[13] ABOUT | Ontario Greenhouse Vegetable Growers. Mysite/Ogvg n.d. https://www.ogvg.com/about (accessed July 4, 2024).
[14] Dinh VN, Leahy P, McKeogh E, Murphy J, Cummins V. Development of a viability assessment model for hydrogen production from dedicated offshore wind farms. Int J Hydrogen Energy 2021;46:24620–31. https://doi.org/10.1016/j.ijhydene.2020.04.232.
[15] Reyes-Bozo L, Fúnez-Guerra C, Luis Salazar J, Vyhmeister E, Valdés-González H, Jaén Caparrós M, et al. Green hydrogen integration in aluminum recycling: Techno-economic analysis towards sustainability transition in the expanding aluminum market. Energy Convers Manage: X 2024;22:100548. https://doi.org/10.1016/j.ecmx.2024.100548.
[16] Lucas TR, Ferreira AF, Santos Pereira RB, Alves M. Hydrogen production from the WindFloat Atlantic offshore wind farm: A techno-economic analysis. Appl Energy 2022;310:118481. https://doi.org/10.1016/j.apenergy.2021.118481.
[17] Li R, Jin X, Yang P, Sun X, Zhu G, Zheng Y, et al. Techno-economic analysis of a wind-photovoltaic-electrolysis-battery hybrid energy system for power and hydrogen generation. Energ Conver Manage 2023;281:116854. https://doi.org/10.1016/j.enconman.2023.116854.
[18] Ozturk M, Dincer I. Development of renewable energy system integrated with hydrogen and natural gas subsystems for cleaner combustion. J Nat Gas Sci Eng 2020;83:103583. https://doi.org/10.1016/j.jngse.2020.103583.
[19] Tebibel H. Methodology for multi-objective optimization of wind turbine/battery/electrolyzer system for decentralized clean hydrogen production using an adapted power management strategy for low wind speed conditions. Energ Conver Manage 2021;238:114125. https://doi.org/10.1016/j.enconman.2021.114125.
[20] Sorgulu F, Dincer I. Analysis and techno-economic assessment of renewable hydrogen production and blending into natural gas for better sustainability. Int J Hydrogen Energy 2022;47:19977–88. https://doi.org/10.1016/j.ijhydene.2022.04.133.
[21] Jang D, Kim K, Kim K-H, Kang S. Techno-economic analysis and Monte Carlo simulation for green hydrogen production using offshore wind power plant. Energ Conver Manage 2022;263:115695. https://doi.org/10.1016/j.enconman.2022.115695.
[22] Lamagna M, Ferrario AM, Astiaso Garcia D, Mcphail S, Comodi G. Reversible solid oxide cell coupled to an offshore wind turbine as a poly-generation energy system for auxiliary backup generation and hydrogen production. Energy Rep 2022;8:14259–73. https://doi.org/10.1016/j.egyr.2022.10.355.
[23] Benalcazar P, Komorowska A. Prospects of green hydrogen in Poland: A techno-economic analysis using a Monte Carlo approach. Int J Hydrogen Energy 2022;47:5779–96. https://doi.org/10.1016/j.ijhydene.2021.12.001.
[24] Groenemans H, Saur G, Mittelsteadt C, Lattimer J, Xu H. Techno-economic analysis of offshore wind PEM water electrolysis for H2 production. Curr Opin Chem Eng 2022;37:100828. https://doi.org/10.1016/j.coche.2022.100828.
[25] Luo Z, Wang X, Wen H, Pei A. Hydrogen production from offshore wind power in South China. Int J Hydrogen Energy 2022;47:24558–68. https://doi.org/10.1016/j.ijhydene.2022.03.162.
[26] Nasser M, Megahed TF, Ookawara S, Hassan H. Techno-economic assessment of clean hydrogen production and storage using hybrid renewable energy system of PV/Wind under different climatic conditions. Sustainable Energy Technol Assess 2022;52:102195. https://doi.org/10.1016/j.seta.2022.102195.
[27] Egeland-Eriksen T, Jensen JF, Ulleberg Ø, Sartori S. Simulating offshore hydrogen production via PEM electrolysis using real power production data from a 2.3 MW floating offshore wind turbine. Int J Hydrogen Energy 2023;48:28712–32. https://doi.org/10.1016/j.ijhydene.2023.03.471.
[28] Superchi F, Mati A, Carcasci C, Bianchini A. Techno-economic analysis of wind-powered green hydrogen production to facilitate the decarbonization of hard-to-abate sectors: A case study on steelmaking. Appl Energy 2023;342:121198. https://doi.org/10.1016/j.apenergy.2023.121198.
[29] Idriss AI, Ahmed RA, Atteyeh HA, Mohamed OA, Ramadan HSM. Techno-economic potential of wind-based green hydrogen production in djibouti: literature review and case studies. Energies 2023;16:6055. https://doi.org/10.3390/en16166055.
[30] Akdağ O. The operation and applicability to hydrogen fuel technology of green hydrogen production by water electrolysis using offshore wind power. J Clean Prod 2023;425:138863. https://doi.org/10.1016/j.jclepro.2023.138863.
[31] Cheng C, Hughes L. The role for offshore wind power in renewable hydrogen production in Australia. J Clean Prod 2023;391:136223. https://doi.org/10.1016/j.jclepro.2023.136223.
[32] Kim A, Kim H, Choe C, Lim H. Feasibility of offshore wind turbines for linkage with onshore green hydrogen demands: A comparative economic analysis. Energ Conver Manage 2023;277:116662. https://doi.org/10.1016/j.enconman.2023.116662.
[33] Komorowska A, Benalcazar P, Kamiński J. Evaluating the competitiveness and uncertainty of offshore wind-to-hydrogen production: A case study of Poland. Int J Hydrogen Energy 2023;48:14577–90. https://doi.org/10.1016/j.ijhydene.2023.01.015.
[34] Nasser M, Hassan H. Techno-enviro-economic analysis of hydrogen production via low and high temperature electrolyzers powered by PV/Wind turbines/Waste heat. Energ Conver Manage 2023;278:116693. https://doi.org/10.1016/j.enconman.2023.116693.
[35] Makepeace RW, Tabandeh A, Hossain MJ, Asaduz-Zaman Md. Techno-economic analysis of green hydrogen export. Int J Hydrogen Energy 2024;56:1183–92. https://doi.org/10.1016/j.ijhydene.2023.12.212.
[36] Giampieri A, Ling-Chin J, Roskilly AP. Techno-economic assessment of offshore wind-to-hydrogen scenarios: A UK case study. Int J Hydrogen Energy 2024;52:589–617. https://doi.org/10.1016/j.ijhydene.2023.01.346.
[37] Benalcazar P, Komorowska A. Techno-economic analysis and uncertainty assessment of green hydrogen production in future exporting countries. Renew Sustain Energy Rev 2024;199:114512. https://doi.org/10.1016/j.rser.2024.114512.
[38] Gado MG. Techno-economic-environmental assessment of green hydrogen and ammonia synthesis using solar and wind resources for three selected sites in Egypt. E-Prime - Adv Electr Eng, Electron Energy 2024;10:100780. https://doi.org/10.1016/j.prime.2024.100780.
[39] Hüner B. Mathematical modeling of an integrated photovoltaic-assisted PEM water electrolyzer system for hydrogen production. Int J Hydrogen Energy 2024;79:594–608. https://doi.org/10.1016/j.ijhydene.2024.07.041.
[40] Park J, Kang S, Kim S, Cho H-S, Heo S, Lee JH. Techno-economic analysis of solar powered green hydrogen system based on multi-objective optimization of economics and productivity. Energ Conver Manage 2024;299:117823. https://doi.org/10.1016/j.enconman.2023.117823.
[41] Magne A, Khatiwada D, Cardozo E. Assessing the bioenergy potential in South America: Projections for 2050. Energy Sustain Dev 2024;82:101535. https://doi.org/10.1016/j.esd.2024.101535.
[42] Najar IN, Sharma P, Das R, Tamang S, Mondal K, Thakur N, et al. From waste management to circular economy: Leveraging thermophiles for sustainable growth and global resource optimization. J Environ Manage 2024;360:121136. https://doi.org/10.1016/j.jenvman.2024.121136.
[43] Shen X, Liu H, Yang X, Zhou X, An J, Yan D. A data-mining-based novel approach to analyze the impact of the characteristics of urban ventilation corridors on cooling effect. Buildings 2024;14:348. https://doi.org/10.3390/buildings14020348.
[44] Vahidhosseini SM, Rashidi S, Hsu S-H, Yan W-M, Rashidi A. Integration of solar thermal collectors and heat pumps with thermal energy storage systems for building energy demand reduction: A comprehensive review. J Storage Mater 2024;95:112568. https://doi.org/10.1016/j.est.2024.112568.
[45] Ma Y, Zhao M, Bai F, Yu R, Liu L, Wang J. Numerical simulation and experimental verification of solar PVT coupled PEM electrolyzer system for hydrogen production. Fuel 2024;365:131323. https://doi.org/10.1016/j.fuel.2024.131323.
[46] Asiaban S, Bozalakov D, Vandevelde L. Development of a dynamic mathematical model of PEM electrolyser for integration into large-scale power systems. Energy Convers Manage: X 2024;23:100610. https://doi.org/10.1016/j.ecmx.2024.100610.
[47] Benghanem M, Almohamadi H, Haddad S, Mellit A, Chettibi N. The effect of voltage and electrode types on hydrogen production powered by photovoltaic system using alkaline and PEM electrolyzers. Int J Hydrogen Energy 2024;57:625–36. https://doi.org/10.1016/j.ijhydene.2023.12.232.
[48] Under Sun Acres Inc. – Your home for greenhouse innovation. n.d. https://undersunacres.com/ (accessed April 29, 2024).
[49] Renewable energy project - Kruger Inc. Energy n.d. https://energy.kruger.com/powerplants/ (accessed April 29, 2024).
[50] Hydrogen | 2G Energy, Inc. n.d. https://www.2g-energy.com/products/hydrogen (accessed April 29, 2024).
[51] Hydrogen. Keen Compressed Gas Co n.d. https://keengas.com/gases/hydrogen/ (accessed April 29, 2024).
[52] Payback Period Calculator n.d. https://www.calculator.net/payback-period-calculator.html (accessed April 22, 2024).
[53] Aghakhani A, Haque N, Saccani C, Pellegrini M, Guzzini A. Direct carbon footprint of hydrogen generation via PEM and alkaline electrolysers using various electrical energy sources and considering cell characteristics. Int J Hydrogen Energy 2023;48:30170–90. https://doi.org/10.1016/j.ijhydene.2023.04.083.
[54] cummins-hydrogen-generation-brochure-20210603.pdf n.d.
[55] cummins-hylyzer-1000-specsheet.pdf n.d.
[56] Reddi K, Elgowainy A, Rustagi N, Gupta E. Techno-economic analysis of conventional and advanced high-pressure tube trailer configurations for

compressed hydrogen gas transportation and refueling. Int J Hydrogen Energy 2018;43:4428–38. https://doi.org/10.1016/j.ijhydene.2018.01.049.
[57] Kuczyński S, Łaciak M, Olijnyk A, Szurlej A, Włodek T. Thermodynamic and technical issues of hydrogen and methane-hydrogen mixtures pipeline transmission. Energies 2019;12:569. https://doi.org/10.3390/en12030569.
[58] EUR Inflation Calculator - Euro (1991-2024) n.d. https://www.inflationtool.com/euro (accessed April 21, 2024).
[59] Inflation Calculator | Find US Dollar's Value From 1913-2024 2024. https://www.usinflationcalculator.com/ (accessed April 19, 2024).
[60] Inflation calculator n.d. https://www.bankofengland.co.uk/monetary-policy/inflation/inflation-calculator (accessed April 21, 2024).
[61] Power Data n.d. https://www.ieso.ca/Power-Data (accessed May 1, 2024).
[62] Parks G, Boyd R, Cornish J, Remick R. Hydrogen station compression, storage, and dispensing technical status and costs. Syst Integr 2014. https://doi.org/10.2172/1130621.
[63] Bank Run Templates. Bank Run Templates n.d. https://bankruntemplates.com/ (accessed May 1, 2024).